EARTHQUAKE SPECTRA

The Professional Journal of the Earthquake Engineering Research Institute

PREPRINT

This preprint is a PDF of a manuscript that has been accepted for publication in *Earthquake Spectra*. It is the final version that was uploaded and approved by the author(s). While the paper has been through the usual rigorous peer review process for the Journal, it has not been copyedited, nor have the figures and tables been modified for final publication. Please also note that the paper may refer to online Appendices that are not yet available.

We have posted this preliminary version of the manuscript online in the interest of making the scientific findings available for distribution and citation as quickly as possible following acceptance. However, readers should be aware that the final, published version will look different from this version and may also have some differences in content.

The DOI for this manuscript and the correct format for citing the paper are given at the top of the online (html) abstract.

Once the final, published version of this paper is posted online, it will replace the preliminary version at the specified DOI.

Active Faulting in Source Region of 2016-2017 Central Italy Event Sequence

Fabrizio Galadini,[a)] Emanuela Falcucci,[a)] Stefano Gori,[a)] Paolo Zimmaro,[b)] M.EERI, Daniele Cheloni,[a)], Jonathan P. Stewart,[b)] M.EERI

ABSTRACT

The Central Italy earthquake sequence produced three mainshocks: **M**6.1 24 August, **M**5.9 26 October, and **M**6.5 30 October 2016. Additional **M**5-5.5 events struck this territory on 18 January 2017 in the Campotosto area. Fault plane solutions for the mainshocks exhibit normal faulting (characteristic of crustal extension occurring in the inner central Apennines). Significant evidence, including hypocenter locations, strike and dip angles of the moment tensors, inverted finite fault models (using GPS, InSAR, and ground motion data), and surface rupture patterns, all point to the earthquakes having been generated on the Mt. Vettore-Mt. Bove fault system (all three mainshocks) and on the Amatrice fault, in the northern sector of the Laga Mountains (portion of 24 August event). The earthquake sequence provides examples of both synthetic and antithetic ruptures on a single fault system (30 October event) and rupture between two faults (24 August event). We describe active faults in the region, their segmentation, and present understanding of the potential for linkages between segments (or faults) in the generation of large earthquakes.

Keywords: faults, segmentation, moment tensor solutions, finite fault models.

INTRODUCTION

The 2016-2017 Central Italy seismic sequence affected a large sector of the central Apennines of Italy. The events struck an area between the regions affected by the 1997 Umbria-Marche and 2009 L'Aquila seismic sequences.

[a)] Istituto Nazionale di Geofisica e Vulcanologia (INGV), Italy
[b)] Department of Civil and Environmental Engineering, University of California Los Angeles, CA, USA

Seismological and geodetic data indicate that the earthquake events were associated with activation of normal faults striking northwest-southeast (NW-SE) and dipping towards the SW (e.g. Tinti et al., 2016; Chiaraluce et al., 2017). The rupture characteristics are compatible with current understanding of the seismotectonics of this part of the central Apennines (e.g. Galadini and Galli, 2000, 2003; Boncio et al., 2004a). Previous field investigations of fault structures in the central Apennines have demonstrated Quaternary (or late Quaternary) activity based on mapped fault displacements across continental sedimentary sequences and associated landforms (e.g. Calamita et al., 2000; Galadini and Galli, 2000, 2003; Tondi, 2000; Boncio et al., 2004a; Galadini et al., 2012; Falcucci et al., 2016). Many of the central Apennine Quaternary normal faults are considered as the surface manifestation of seismogenic sources potentially responsible for **M**6.5-7 earthquakes. This is based on fault system lengths at the surface often in the order of 20-30 km, which are comprised of segments that are up to approximately 10 km in length. These hypotheses have been verified by the recent seismic sequences. We show here that the faults that produced this seismic sequence occurred on known active normal faults of this type.

In this paper, we describe the fault structures on which the mainshock events in this earthquake sequence occurred and the active faults surrounding the epicentral area. We provide geometric and kinematic parameters for these fault systems. Such information can be used for regional active tectonics and stress analyses, as well as for seismic hazard and risk analyses. In this paper the terms *fault* or *fault system* refer to seismogenic structures comprising one segment (*fault*) or multiple segments (*fault system*) that are part of the same geologic feature, and which are capable of rupturing partially or fully together during a single event. As used here, a *fault segment* is a continuous feature within a fault system.

We also present specific source information in the form of hypocenter locations, finite fault models useful for distance calculations, and aftershock patterns. We do not describe the surface rupture produced by the event sequence, which is described and analyzed in detail in a companion paper (Gori et al. 2018, this issue).

GEOLOGICAL FRAMEWORK

The Apennine belt represents the “spine” of the Italian Peninsula and results from the complex interaction between the Africa and Europe plates, and the Adria microplate. The formation of the central portion of the chain started in the Oligocene, when a compressive

front began to “squash” and displace Mesozoic and Cenozoic marine carbonate sequences (e.g. Ciarapica and Passeri, 1998; Patacca et al., 2008; Cosentino et al., 2010). The front superposed different tectonic units and advanced progressively towards the east and north-east through thrust-and-fold systems that become progressively younger to the east. Migration of the thrust front occurred as a result of successive deformation events, which are expressed as different foredeep and thrust-top basins that are nestled in between the fronts (e.g. Cipollari et al., 1999; Centamore and Rossi, 2009; Cosentino et al., 2010; 2017).

Since the Pliocene, when compression was deforming the present Adriatic domain, the Tyrrhenian area (interpreted as a back-arc basin) and the inner sectors of the central Apennines has experienced tectonic extension (Malinverno and Ryan, 1986; Cavinato et al., 1994; Cavinato and De Celles, 1999; Cosentino et al., 2010). The extensional tectonics nucleated a series of NW-SE trending, i.e. chain-parallel, normal fault systems, which displaced the older compressive structures (Figure 1a). The compression-extension tectonic pair migrated east-northeastwards (e.g. Galadini and Messina, 2004; Fubelli et al., 2009; Carminati and Doglioni, 2012). The entire process occurred contemporaneously with chain uplift (e.g. Galadini et al., 2003), which amounted to about 1000 m over the Quaternary (e.g. D’Agostino et al., 2001).

Evidence of ongoing extension of the central Apennine chain is provided by:

1) Seismicity, with minor-to-major earthquakes on NW-SE trending extensional ruptures, including the **M**6.1, 6 April 2009 L’Aquila earthquake (Chiarabba et al., 2009; Valoroso et al., 2013) and the 2016-2017 seismic sequence (e.g. Tinti et al., 2016, for the sequence between 24 August and 30 October 2016; Gruppo di Lavoro INGV sul terremoto di Visso, 2016; http://cnt.rm.ingv.it/event/8863681, last accessed 10/12/2017; Cheloni et al., 2017);

2) Geodetic data, with GPS time series indicating 2-3 mm/yr extension in the NE-SW direction (D’Agostino et al., 2011; Devoti et al., 2011; 2017);

3) Borehole breakout data, showing minimum horizontal stress oriented perpendicular to the belt (Montone and Mariucci, 2016); and

4) Geological data, indicating activity of normal faults and fault systems during the Quaternary (e.g. Galadini and Galli, 2000; Boncio et al., 2004a; Roberts and Michetti, 2004), as well as paleoseismological evidence of activity on central Apennine major

normal faults during historical times, nucleating **M**6.5-7 events. Notable among these events are the 1703 seismic sequence, with two major shocks in the Norcia (14 January) (Galli et al., 2005) and the L'Aquila (2 February) (Moro et al., 2002) sectors (Figure 1b) and the 1915 event in the Fucino basin (e.g. Ward and Valensise, 1989; Michetti et al., 1996; Galadini and Galli, 1999).

The following sections describe regional faults in the epicentral region of the 2016-2017 seismic sequence, with an emphasis on those faults to which the 24 August, 26 and 30 October 2016 mainshock events are attributed.

REGIONAL FAULTS OVERVIEW

The Apennine chain in Central Italy has series of normal faults that accommodate regional extension. Varying amounts of information are available for these faults from field studies, trenching, and historical data. A critical issue for hazard characterization is what combination of faults, fault segments, and fault systems can rupture in a single event. In the Central Appennine region, some seismogenic structures consist of multiple discrete segments that can rupture together, as was the case for example with the Mt. Vettore-Mt. Bove fault system that was primarily responsible for the mainshocks that occurred in 2016. What is less clear is when rupture can occur between fault systems, which was also a feature of the 24 August 2016 event (it is beyond the scope of this document to resolve such questions in a general sense). Under a seismotectonic perspective, ruptures of a number of fault systesms in very short time spans (from few minutes to several days from one another), have occurred over the past millennium in the central and southern Apennine during complex seismic sequences. This is the case of the 1349, 1456, and 1703 earthquake sequences. This demonstrates that kinematically independent and even not contiguous fault systems activated in the past for various possible reasons (i.e. stress transfer, dynamic triggering, fluids migration) and that a similar scenario can occur again in an undefined future.

As for the 24 August event, the rupture of the two faults did not released a seismic moment associated to the rupture of a single large fault but to the single ruptures of the two slip patches.

In this section, we briefly describe faults and fault systems in the broader region of the 2016-2017 earthquake sequence. This summary has two objectives:

1. To synthesize fault attributes from prior work that are useful in source models, for example as used in seismic hazard analyses;

2. To establish the context, from a faulting perspective, that allows the significance of the 2016 earthquake sequence to be understood and appreciated.

We first examine major regional faults, and then focus more specifically on the faults that produced the 2016 main events of the sequence (Mt. Vettore-Mt. Bove fault system and Amatrice fault). As shown in Figure 1b, additional significant faults in the region include the Colfiorito and Sellano basin faults, the Norcia fault system and the Upper Aterno valley-Paganica fault system. Two further structures are also shown, namely the Leonessa fault and the Monti Gemelli-Montagna dei Fiori fault, as normal faults that appear to be inactive (i.e. they are not able to generate surface rupturing earthquakes, that is **M**<6±0.2; Falcucci et al., 2016). Table 1 presents selected characteristics and references for each of these regional faults. More details about geological evidence of past activity of the faults reported in Figure 1b and historical seismicity associated with each fault are provided in GEER (2017).

Beginning from the north end of the region shown in Figure 1b, the Colfiorito and Sellano basin faults were responsible for the seismic sequence that struck the Umbria-Marchean region in September-October 1997 (e.g. Pantosti et al., 1999; Cello et al., 2000; Calamita et al., 2000; Vittori et al., 2000; Chiaraluce et al., 2005; Barchi e Mirabella, 2009; Ferrarini et al., 2015) with three mainshocks of **M**5.6-to-6. These faults are *en-echelon* arranged with dextral step-over. Based on geological and historical data, we consider multi-fault ruptures on these faults to be unlikely, that is, each fault ruptures separately with earthquakes of up to M6±0.2 (Messina et al., 2002), as occurred in 1997. Moreover, as shown in Figure 1b, due to the large separation and geological evidence about different recent kinematic behavior, simultaneous rupture with the neighboring Mt. Vettore-Mt. Bove fault system or the Norcia fault system to the south is considered unlikely.

Five moderate-to-large magnitude seismic events occurred in the past millennium in the Norcia basin area: in 1328, 1703, 1730, 1859, and 1979. Based on damage distributions (Galadini et al., 1999), the pre-20th century events could be attributed to the activation of the whole Norcia fault system, as in 1703, or to single segments of the structure. The fault system consists of four major segments, as shown in Figure 1b. The **M**6.9 1703 event produced damage across the entire Norcia sector, suggesting synchronous activation of the whole seismogenic fault system. This is also supported by paleoseismological investigations,

which find evidence of surface ruptures with displacements consistent with the reported magnitude (Galli et al., 2005). Other historic events (such as the 1328, 1730, 1859, 1979 seismic events) have likely ruptured single fault segments in earthquakes with **M** ≤ 6.5 (Galadini et al., 1999).

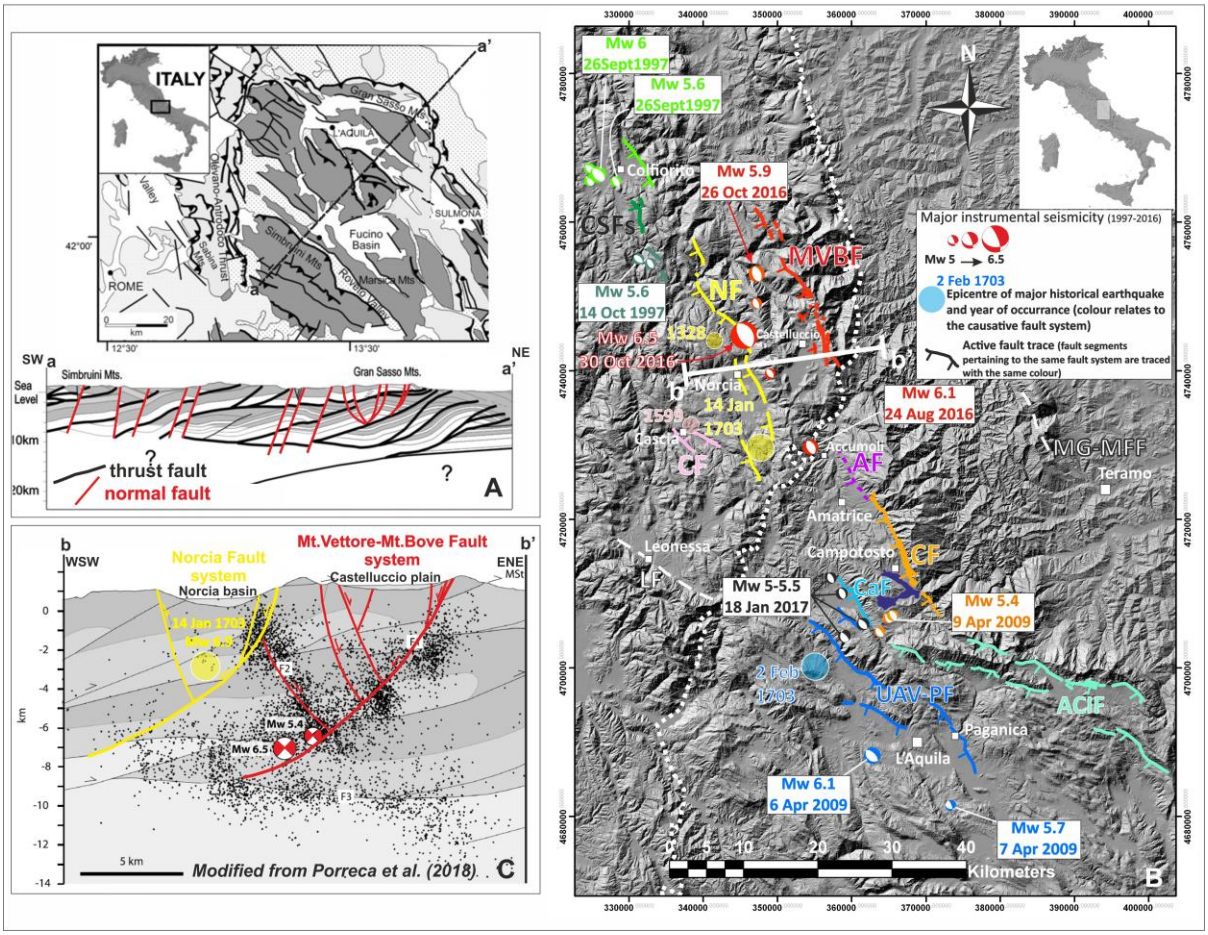

Figure 1. (a) Schematic geological setting of the central Apennines (upper panel) and cross-section showing the relationship between the compressive tectonic structures and the Pliocene-Quaternary normal faults (modified from Falcucci et al., 2015); (b) Map showing active faults and fault systems discussed in this section and locations of large seismic events in the region since 2009, as well as historical seismicity. Faults: Colfiorito and Sellano basin faults, CSFs; Mt. Vettore-Mt. Bove fault system, MVBF; Norcia fault system, NF; Cascia fault, CF; Amatrice fault, AF; Campotosto fault, CF; Capitignano fault, CaF; Upper Aterno Valley-Paganica fault system, UAV-PF; Leonessa fault, LF; Monti Gemelli-Montagna dei Fiori fault, MGMFF. The Olevano-Antrodoco-Sibillini inactive thrust system is defined by the white dotted line. The trace of the geological cross-section b-b' shown in (c) is marked by the white line. (c) Geological cross-section, modified from Porreca et al. (2018), showing the deep structural setting of the epicentral area of the 30 October 2016 mainshock, in relation with the aftershock sequence (black dots).

Located at the south end of Figure 1b is the upper Aterno valley, i.e. the L'Aquila region. The Upper Aterno Valley-Paganica fault system consists of four NW-SE normal fault segments. The Paganica segment of this fault system generated the 2009 earthquake (**M**6.1)

(e.g. Chiaraluce, 2012; Valoroso et al., 2013). The seismogenic behavior of the fault system is complex. Current knowledge indicates that it can rupture both entirely, generating **M**~6.7 earthquakes, as on 2 Feb. 1703, and partly, with single segments generating **M**~6, as in 2009.

Two faults shown in Figure 1b are considered inactive, that is, they are unable to produce surface rupturing earthquake (**M**6±0.2, threshold magnitude of surface faulting earthquakes for Apennine extensional faults; Falcucci et al., 2016): the Leonessa fault and the Monti Gemelli-Montagna dei Fiori fault. As explained further in GEER (2017), the Leonessa fault was possibly active during the late Pliocene-lower Early Pleistocene and its activity ended or strongly reduced during the Middle Pleistocene-late Quaternary. There are no historical earthquakes associated with this fault. The Montagna dei Fiori-Monti Gemelli fault is associated with a NW-SE trending anticline related to an ancient thrust active between the Late Messinian and the Lower Pliocene. Probably the normal fault was active during Miocene pre-thrusting and thrusting phases (Scisciani et al., 2002; Storti et al., 2016; 2017). Despite the presence of a sporadically exposed fault scarp, geological evidence suggests that the Montagna dei Fiori-Monti Gemelli fault is inactive in the Quaternary. Strong historical earthquakes cannot be associated to this fault. Minor events of low magnitude sometimes occur in the area. However, the relationship of these events with the fault is unclear.

The following sub-sections describe active faults in the region that produced the 2016 mainshocks, namely the Mt. Vettore-Mt. Bove fault and the Amatrice fault. Each sub-section describes geological data, mainly based on the criteria from Falcucci et al. (2016), and reviews historical seismicity, which collectively provide the basis for inferences of current activity. Data on past earthquakes and the damage distribution have been derived from Rovida et al. (2016). Table 1 summarizes main seismogenic characteristics of these faults.

Table 1. Summary of the kinematic, geometric, and seismogenic characteristics of the faults located in the region. Rake angles for all considered faults (normal kinematics) are ~ 90°.

Fault/Fault system	No. segments	Associated historical/recent earthquakes	Average dip (°)	Surface length (km)	Upper and lower seismogenic depth (km)	Maximum expected magnitude (uncertainty)[1]	Previously modeled as seismogenic source[2]	Slip rate (mm/yr)	Recurrence time (years)
Mt. Vettore-Mt. Bove fault system	3	Aug 2016 (**M**6.1) Oct 2016 (**M**5.9 and **M**6.5)	45	27	Upper: 0 Lower: 10	**M**6.7 (±0.1)	BEA04: Y (1) AKI09: Y (1) DISS: D	0.36- 0.62 (min.)	ca. 4500 (max.)
Campotosto fault	1	-	45	20	Upper: 0 Lower: 10	**M**6.5 (±0.1)	BEA04: Y (1) AKI09: Y (1) DISS: D	0.7-0.9	ca. 7500 (max.)
Amatrice fault	1	Oct 1639 (**M**6.2) Aug 2016 (**M**6.1)	45	8	Upper: 2 Lower: 10	**M**<6.0 (±0.2)	BEA04: Y (1) AKI09: N DISS: D	-	400 (**M**6.0)
Colfiorito and Sellano basins faults	3	Apr 1279 (**M**6.2) Sep 1997 (**M**6.0) Oct 1997 (**M**5.6)	45	8	Upper: 2 Lower: 10	**M**<6.0 (±0.2)	BEA04: Y (2) AKI09: Y (1) DISS: Y (3)	-	700 (**M**6.0)
Norcia fault system	4	Dec 1328 (**M**6.5) Jan 1703 (**M**6.9) May 1730(**M**6.0) Aug 1859 (**M**5.7) Sep 1979 (**M**5.8)	45	31	Upper: 0 Lower: 10	**M**6.9 (±0.1)	BEA04: Y (2) AKI09: Y (1) DISS: C	0.25-1.15	1700-1900 (**M**6.9)
Upper Aterno Valley-Paganica fault system	4	Nov 1461 (**M**6.5) Feb 1703 (**M**6.7) Oct 1762 (**M**5.5) Apr 2009 (**M**6.3)	45	27	Upper: 0 Lower: 10	**M**6.7 (±0.2)	BEA04: Y (3) AKI09: Y (2) DISS: C (2), Y (2)	0.47-0.86	500 (**M**6-6.2) 850-1700 (**M**6.7)
Leonessa fault	1	-	60	20	Upper: 2 Lower: 10	**M**<6.0(±0.2)	BEA04: N AKI09: N DISS: C	-	-
Montagna dei Fiori-Monti Gemelli fault	1	-	60	15	Upper: 2 Lower: 10	**M**<6.0(±0.2)	BEA04: N AKI09: N DISS: C	-	-

[1]Based on expert judgement.

[2] BEA04 = Boncio et al. (2004a); AKI09 = Akinci et al. (2009); DISS = DISS Working Group (2015); Y = Modeled as individual segment; D = Debated source; C = Modeled as composite source; N = Not modeled; (#) = Number of segments (if modeled as individual segments).

MT. VETTORE-MT. BOVE FAULT SYSTEM

Geological evidence of recent activity

The Mt. Vettore-Mt. Bove normal fault system strikes NNW-SSE to NW-SE and dips WSW to SW, and can be detected for a length of about 27 km (Figure 1b and c). It is characterized by a prominent fault scarp exposed in the SW carbonate slopes of the Sibillini Mts. (Figure 2). Based on available geomorphologic evidence, the fault was recognized as active by several authors (e.g. Calamita and Pizzi, 1992; Cello et al., 1997; Galadini and Galli, 2000; 2003; Boncio et al., 2004a) prior to the 2016 earthquake sequence.

Only one intermontane basin can be associated with this fault, i.e. the Castelluccio plain, close to the southernmost end of the fault. The basin is bordered by some of the fault splays located in the piedmont area of Mt. Vettore, one of which has been the object of paleoseismological investigations, described below. However, the origin of the Castelluccio plain cannot be entirely related to fault activity, since geomorphologic traces of karstic processes that contributed to the plain evolution are widespread, such as swallow holes, dolines, and local endorheic hydrographic nets. The geomorphic aspect of the Castelluccio plain seems to resemble that of a *polje* (i.e. a large karstic depression) and was defined by Principi (1911) as the source area of part of the groundwater in the Norcia basin (due to groundwater flow along karstic pathways).

The most impressive fault scarp (fault line scarp at places) is represented by the “Cordone del Vettore” (Figures 2a, 2b), located at about 2,000 m above sea level (asl) in the uppermost portion of the slope (Calamita and Pizzi, 1992; Coltorti and Farabollini, 1995; Cello et al., 1997; Pizzi et al., 2002; Pizzi and Galadini, 2009). Along the bedrock scarp, the exposed fault plane displaces the carbonate rocks, which are overlain by a thin and discontinuous cover of debris on the hanging wall. A less prominent bedrock fault scarp occurs at lower elevation along the same slope of Mt. Vettore (white arrow in Figures 2a and 2b). This lower fault plane places the carbonate bedrock into contact with carbonate bedrock and with slope deposits of Late Pleistocene-Holocene age (Coltorti and Farabollini, 1995).

Further evidence of recent fault activity is provided by the displacement of a wide alluvial fan filling the northern sector of the Castelluccio plain (Figure 3). The displacement is due to the motion of a further fault strand, parallel to the aforementioned main splays on the slopes (Galadini and Galli, 2003). The alluvial fan is comprised of several depositional units dated between 23,000 and 3,200 BP. The motion of this fault splay, paleoseismologically

investigated in 1999 (Figures 3a and 3b), and the related scarp formation can be attributed to a time span ranging between the Late Pleistocene-Holocene and 3,800-3,200 years BP, resulting in a slip rate between 0.36 and 0.62 mm/yr. Surface faulting (vertical offset up to about 20 cm) along the splay trenched in 1999 has been observed after the 30 Oct 2016 event (Figure 3c) (Civico et al., 2018; Villani et al., 2018; Gori et al., this issue). Huang et al. (2017) present an alternative interpretation of a deep-seated landslide with a head scarp at the preexisting fault scarp along the Mt. Vettore slope, which if present, would significantly influence the long-term fault slip rate estimated using geological observations and paleoseismology (Galadini and Galli; 2003). However, Galadini and Galli (2003) trenched within the flat Castelluccio plain, where no landsliding can occur. Hence, the slip rates presented in Galadini and Galli (2003) are unlikely to have been affected by landslide movements.

Associated seismicity

While the last fault activation is traced to the beginning of the first millennium B.C. based on paleoseismic data (Galadini and Galli, 2003; Galli et al., 2008), no historical earthquakes can be associated with this fault. It is for this reason that the fault was considered "silent" prior to the 2016-2017 sequence by Galadini and Galli (2000), meaning that the elapsed time since the last significant event is many centuries/some millennia (minimum elapsed time 1,300-1,500 years) (Galadini and Galli, 2003).

Seismogenic interpretation

Despite the lack of recent activity, the aforementioned paleoseismic evidence of surface rupture led Galadini and Galli (2000) to suggest that the Mt. Vettore-Mt. Bove fault system represents the superficial expression of a seismogenic source potentially responsible for **M**6.5 earthquakes. Indeed, the geologic and geomorphologic characteristics of the Mt. Vettore-Mt. Bove fault system are similar to those of other well-known active faults in the central Apennines. For this reason, the 2016 earthquake sequence is not surprising in terms of the seismogenic characteristics of this fault and in general of the Apennines. Smeraglia et al. (2017) reach a similar conclusion, based on micro-structural analyses along the fault plane, at the southernmost sector of the structure, which showed that the fault slipped seismically during past earthquakes.

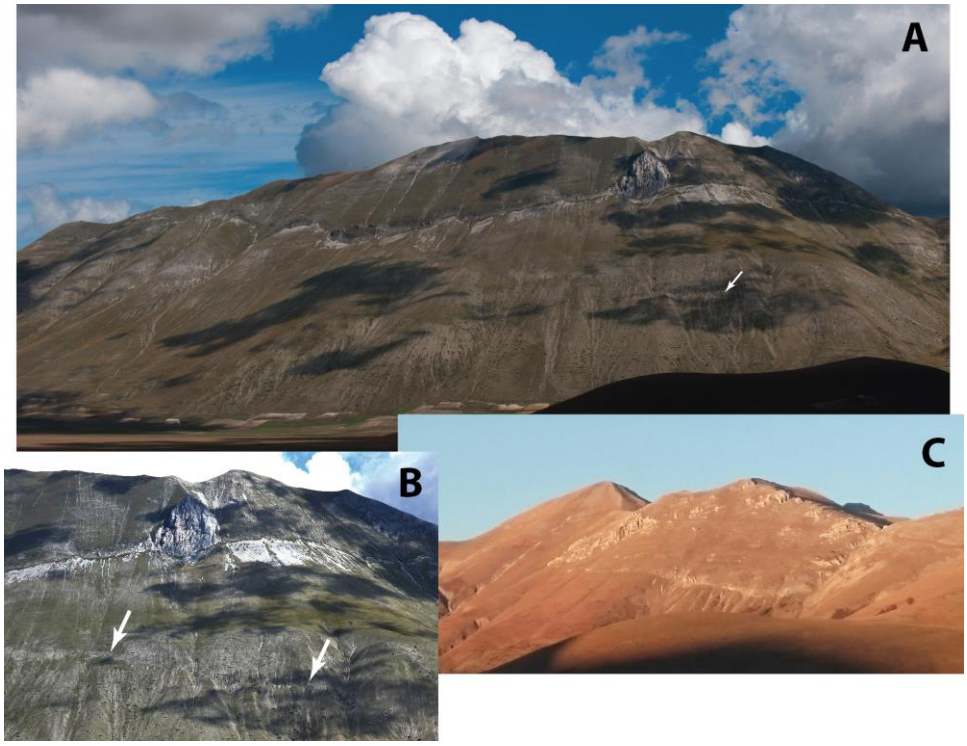

Figure 2. (a), (b) Mt. Vettore-Mt. Bove fault system: bedrock fault scarps along the SW slope; the uppermost scarp is known as "Cordone del Vettore"; the white arrows indicate the bedrock scarp located in the middle sector of the slope; (c) bedrock fault scarp along the western slope of Palazzo Borghese, between Mt. Porche and Mt. Argentella, NW of Mt. Vettore.

Based on the fault geometry as expressed at the surface, the Mt. Vettore-Mt. Bove fault system was proposed as a NW-SE trending and SW dipping seismogenic source by Galadini and Galli (2000, 2003). More recent investigations proposed that the source has a 27-km-long superficial expression, consistent with an expected maximum magnitude of ~6.7 (Falcucci et al., 2016).

A structural interpretation of the Mt. Vettore-Mt. Bove seismogenic source posits the system as negatively inverting the Sibillini thrust ramp (Bonini et al., 2016; Scognamiglio et al., 2018) or even an older structure (e.g. Di Domenica et al., 2014; Falcucci et al., 2018). An alternative interpretation of the faulting from the October 30 2016 mainshock suggests that a significant part of the coseismic slip (and seismic moment release) involved an inferred low angle structure transverse to the Mt. Vettore-Mt. Bove fault system that comprised the lateral ramp of the thrust (Scognamiglio et al., 2018). Similarly, Pizzi et al. (2017) proposed that the lateral ramp of the Sibillini thrust acted somehow to separate the rupture of the October 30 2016 mainshock from that of the August 24 2016 mainshock.

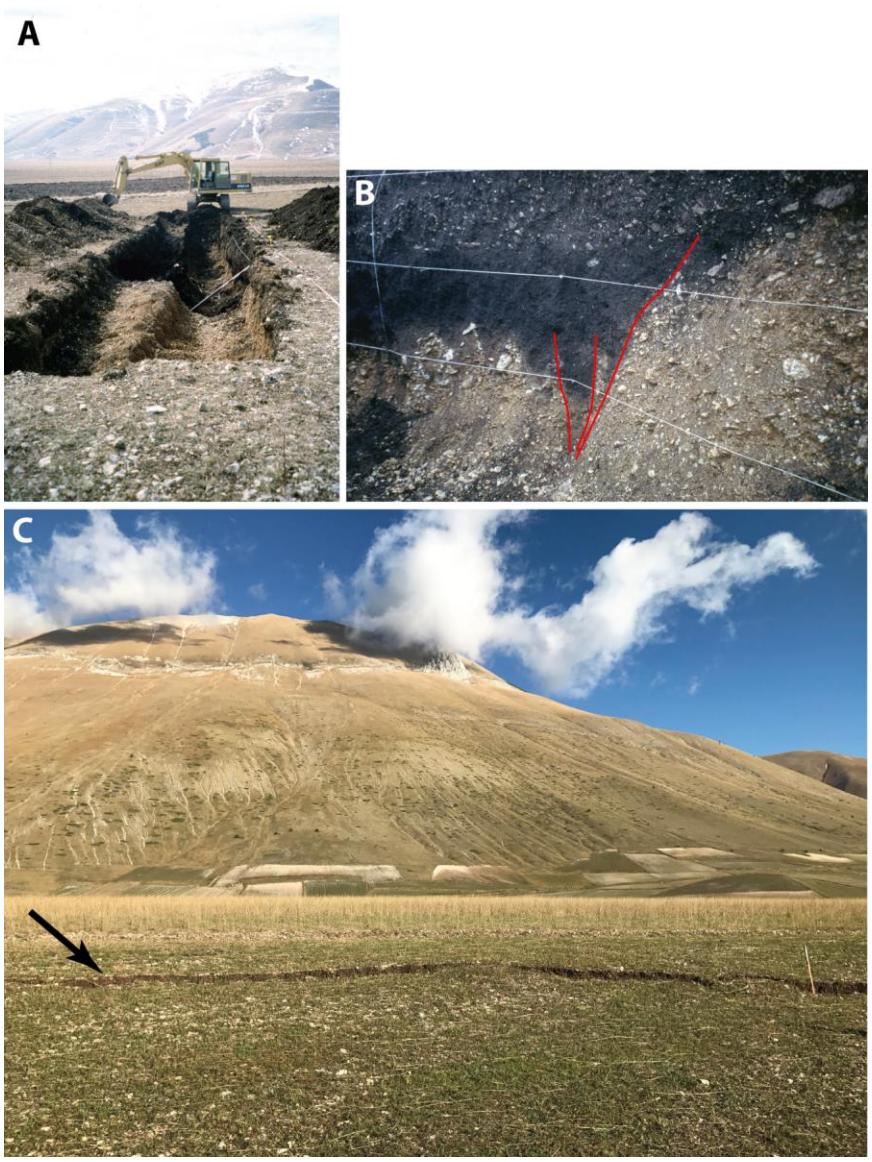

Figure 3. Castelluccio plain: (a) view of one of the paleoseismological trenches excavated in 1999 by Galadini and Galli (2003); (b) NW trench wall: the fault places Late Pleistocene-Holocene gravels in contact with Holocene paleosol and colluvium; (c) 10-20 cm surface displacement caused by the 30 October 2016 earthquake (**M**6.5) along the fault splay trenched in 1999.

Despite the prior studies on this fault system, it was not considered as an individual seismic source for this region by the DISS Working Group (2015). It was considered as a "debated source" (ITDS002), which means a potential seismogenic source proposed in the literature but not considered reliable enough to be included in the database. Other source models for this portion of Italy include the Mt. Vettore-Mt. Bove fault system within a map of seismogenic boxes (Boncio et al., 2004a) and as an individual source (Akinci et al., 2009) (Table 1).

LAGA MTS. FAULTS: THE AMATRICE AND CAMPOTOSTO FAULTS

Geological evidence of recent activity

As shown in Figure 1b, the western slope of the Laga Mts. is affected by two aligned normal faults: the Amatrice fault to the north, and the Campotosto fault to the south, striking NW-SE, dipping towards SW. These faults border two geomorphologic domains: the Amatrice basin to the north and the Campotosto plateau to the south. Although apparently located along the same fault system, the two areas have different geomorphologic characteristics (Galadini and Messina, 2001; Boncio et al., 2004b). The Amatrice area is similar to numerous other basins of the central Apennines, having experienced lacustrine and alluvial deposition during the Quaternary (Cacciuni et al., 1995). In contrast, the Campotosto plateau is a highland containing late Quaternary units made of lacustrine, alluvial and debris deposits typical of piedmont areas (e.g. Galadini and Messina, 2001).

Different from most other central Apennine Quaternary faults, the two fault scarps are carved onto a relatively weak bedrock known as Laga flysch, which consists of arenaceous and clayey successions. In spite of this, the major fault scarp and scarps associated with synthetic minor splays of the Campotosto fault are visible at the base and along the Laga Mts. slope (Figure 4).

The two faults have been defined as tectonically active in the Quaternary (Galadini and Messina, 2001). Quaternary activity in the Amatrice sector may be related to the formation of the related intermontane basin from extension, likely with processes similar to those of the other Apennine depressions, even if its origin may be pre-Quaternary (Falcucci et al., 2018). The oldest sediments and related landforms are displaced and tilted (Cacciuni et al., 1995). However, the top of the Early Pleistocene units is only displaced by 20-30 m (Galadini and Messina, 2001), suggesting that tectonic activity may have significantly decreased during the Quaternary, such that the fault has to be considered inactive during the late Quaternary or affected by displacement events with very low vertical offset (Galadini and Messina, 2001).

Alluvial and lacustrine deposits not older than the Late Pleistocene are present along the southern fault section (Campotosto plateau), in the piedmont area of Laga Mts. These deposits overlie the Miocene flysch. This kind of deposition also occurred during the Holocene (Galadini and Galli, 2003). Late Quaternary deposits in the Campotosto area are

significantly displaced by the Campotosto fault. A vertical displacement larger than 20 m affects an alluvial terrace formed during the upper Late Pleistocene and displacement of alluvial deposits of age 8,000 years BP has been observed (Galadini and Galli, 2003; Figure 4d). Along the Vomano valley, south of the Campotosto plateau, a succession of relict paleo-landsurfaces was identified on the hanging wall of the fault. The absence of similar landforms in the footwall was interpreted as the result of tectonic lowering of the hanging wall and relative minor uplift of the footwall (Galadini and Messina, 2001). This type of terracing up to an elevation close to the present valley bottom suggests the persistence of recent (late Quaternary) tectonic processes (Galadini and Messina, 2001).

The relative lack of significant late Quaternary slip on the Amatrice fault contrasts with evidence of surface activity during the Late Pleistocene and the Holocene on the Campotosto fault. The different ages of fault activity indicate a sort of along-fault migration of fault activity during the Quaternary, from north to south (Galadini and Messina, 2001).

Associated seismicity

An historic earthquake sequence began on 7 October 1639 (**M**6.2; Castelli et al., 2016). Only a single account describes the events, from a writer in Rome, far from the epicentral area. That writer gathered oral reports from witnesses about the coseismic effects. Based on this account, the highest damage has been estimated as intensity I 10 MCS at one location and intensity I 9-10 MCS at 12 locations. Damage at Amatrice was listed with I 9 MCS. Most of the coseismic effects occurred in the Amatrice basin; little information is available about damage in surrounding areas.

Considering the significant impact the earthquake had in the Amatrice area and the magnitude attributed to the 1639 mainshock, the 24 August 2016 earthquake has been compared to the 1639 event. However, because the damage from the 1639 event was mostly localized in Amatrice, and many historical buildings within the city did not suffer damage, it may be that the magnitude of the 1639 event is overestimated. Compounding the problem is the excessive emphasis given to the historical damage descriptions from only a single written source and the likely accumulation of damage across events within an earthquake sequence and the unknown damage from the mainshock (Castelli et al., 2002). We note that the 1639 event produced no strong damage in Norcia and surrounding areas, whereas the 24 August 2016 event caused significant damage north of the Amatrice basin.

Seismogenic interpretation

Geological data suggest the presence of distinct normal faults along the Laga Mts. SW slope, one in the Amatrice basin to the north and one in the Campotosto plateau and the Vomano valley to the south. These faults, although apparently contiguous, appear to have differing tectonic activity and seismotectonics. The only historical seismicity is related to the 1639 event that struck Amatrice, with little damage to the surrounding areas, which suggests activation of the Amatrice fault. The magnitude attributed to the earthquake (6.2) results presumably from cumulative damage from the seismic sequence and possibly from an exaggeration in the description of the damage by the single written source, resulting in an overestimation of the actual 1639 mainshock magnitude. Recent seismicity also supports characterization of the faults as distinct seismogenic sources, since earthquakes related to the 2009 sequence and those that occurred on 18 January 2017 were mainly associated with the Campotosto fault, while the 24 August 2016 events occurred on the Amatrice fault.

The Amatrice fault is considered active from the standpoint of producing earthquakes that can generate strong shaking, but not large enough to produce surface faulting (e.g. Falcucci et al., 2016 and references therein). Events occurring on this structure (presumably the 1639 earthquake), or on this fault in combination with the Mt. Vettore-Mt. Bove fault system to the north (2016) do not appear to cause surface faulting along the Amatrice fault, as indicated by the surveys following the recent event (Emergeo, 2016) and by the investigations on the geomorphic features related to the long-term geological evolution of the Laga Mts. western slope (Galadini and Messina, 2001). The maximum magnitude of events rupturing this fault on its own, without neighboring faults as in 2016, is therefore $< 6 \pm 0.2$.

The rupture on both the Amatrice fault and the Mt. Vettore-Mt. Bove fault system in the 24 August 2016 event is an important observation being considered by different research groups (e.g. Lavecchia et al., 2016; Tinti et al., 2016; Cheloni et al., 2017). Importantly, the two slip patches are clearly separated from one another and the total seismic moment released during the event is the sum of the seismic moments released by the two distinct ruptures and not the seismic moment released by a single large fault comprising the two ruptures.

There is no record of historical events on the Campotosto fault, although geomorphologic and paleoseismological evidence indicates Holocene activity (Figure 4). This suggests that the structure should be considered active (attributes in Table 1), with a length that indicates it can produce earthquakes up to about **M**6.5 (Falcucci et al., 2018).

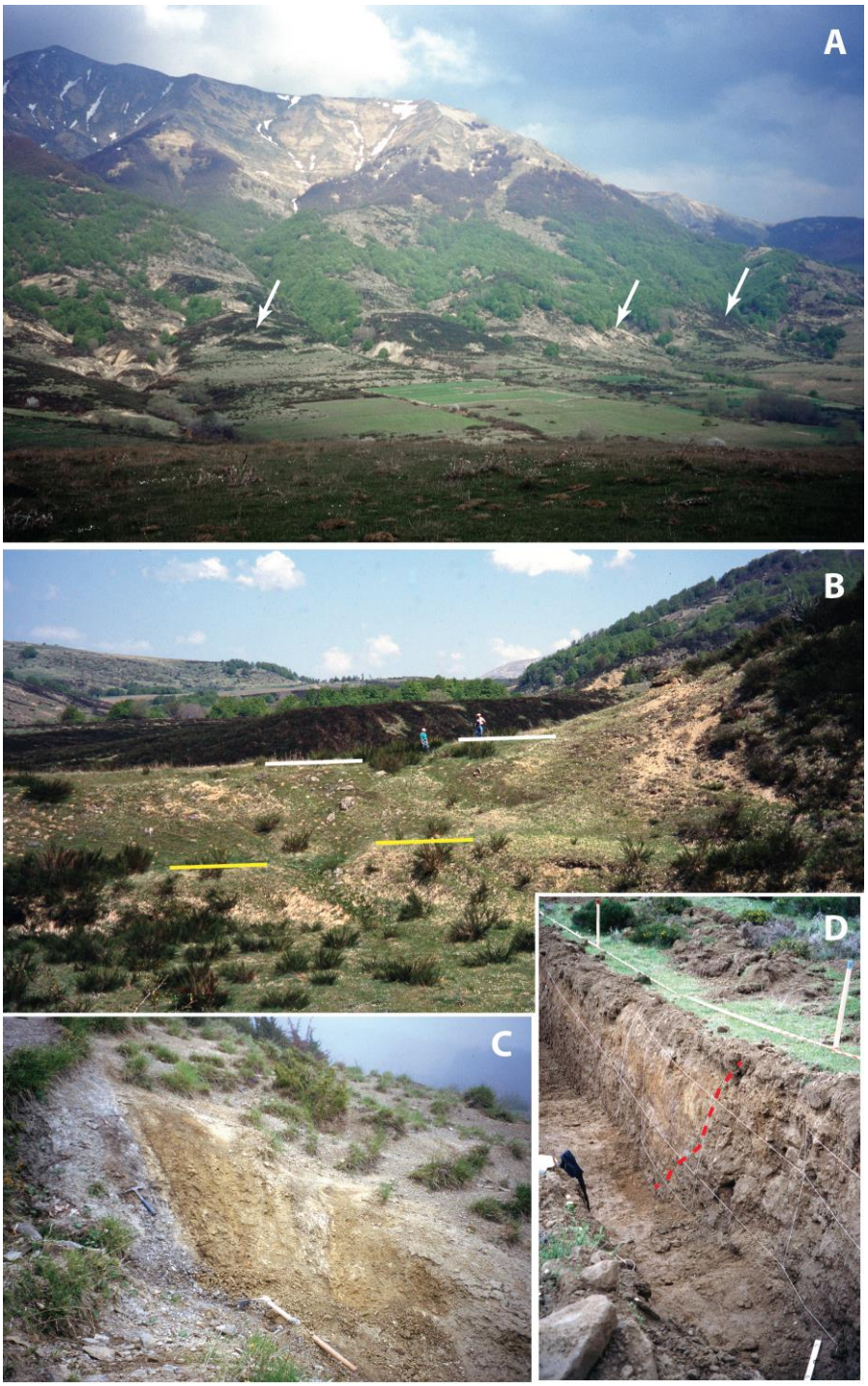

Figure 4. (a) Panoramic view of the Campotosto fault scarp; the arrows indicate places where fault scarps in the arenaceous bedrock have been detected; (b) Holocene terraces (white and yellow lines) displaced by the Campotosto fault; (c) fault plane placing the clayey-arenaceous Laga flysch in contact with colluvium probably deposited during the Late Pleistocene; (d) panoramic view of the trench excavated in 1998 across the Campotosto fault by Galadini and Galli (2003); the fault places the arenaceous bedrock of the Laga flysch in contact with colluvial units of Holocene age.

Interpretations different from those presented here are provided by Boncio et al. (2004b) and Akinci et al. (2009). Boncio et al. (2004b) consider the Laga Mts. faults as the expression

of a single, unsegmented structure (Mt. Gorzano). Akinci et al. (2009) consider only the Campotosto fault as a source capable of producing strong earthquakes; they justify this hypothesis by neglecting the activity from the 1639 earthquakes with the argument that the magnitudes are smaller than those reported in seismic catalogues, and hence the event represents background seismicity. Bigi et al. (2012) propose another hypothesis in which the surficial Campotosto fault is not directly connected with the seismogenic fault at depth, the latter ending updip against a thrust plane inherited from the preceding compressive tectonic phase. This hypothesis seems not to be in agreement with the 18 January 2017 events along the Campotosto fault, whose ruptures cross-cut unhindered the supposed thrust plain (Falcucci et al., 2018).

Although the DISS database (DISS Working Group, 2015) reported a fault in the Laga Mts. area (within the debated seismogenic source ITDS073), single seismogenic sources were not defined. However, this area is partly included in composite source ITCS028.

MOMENT TENSOR AND AFTERSHOCK PATTERN

In this and the following section, we present evidence for the mainshock events having occurred on the Mt. Vettore-Mt. Bove fault system and the Amatrice fault. Additional evidence of this is provided by the surface rupture data provided by Gori et al. (this issue) and references therein.

Between 24 August and 30 October 2016, 17 events with **M**>4.2 were recorded by the Italian National Seismic Network (Rete Sismica Nazionale, RSN; www.gm.ingv.it/index.php/rete-sismica-nazionale/, last accessed 2 October, 2017) owned by the Italian Institute of Geophysics and Vulcanology (Istituto Nazionale di Geofisica e Vulcanologia, INGV). Table 2 shows parameters and locations of the six largest-magnitude events from that sequence. Using event-type classification procedure by Wooddell and Abrahamson (2014), we identified three mainshocks: (1) 24 August **M**6.1, (2) 26 October **M**5.9, and (3) 30 October **M**6.5 (bold entries in Table 2). Data for the 24 August **M**6.1 and 26 October **M**5.9 events are from Cheloni et al. (2017). Finite fault information for the 30 October **M**6.5 events were evaluated in this study (Section *Finite Fault Models*). All other data presented in Table 2 are from http://cnt.rm.ingv.it (last accessed 3 April, 2017).

Figure 5 shows focal mechanisms for each mainshock event and **M**>5 aftershocks. Each mainshock involved normal slip on faults striking NW-SE and dipping to the SW. Specifics

for each event are given in Table 2. The focal mechanism of the 24 August 2016 event occurred in a gap between the mapped Mt. Vettore-Mt. Bove fault system to the north and the Amatrice fault to the south. It is possible that the focus of this event actually occurred at the northernmost tip of the Amatrice fault. The strike of the fault from the moment tensor is generally consistent with the orientation of both faults. The hypocenter locations, slip directions, and surface rupture suggest that the 26 and 30 October events occurred on segments of the Mt. Vettore-Mt. Bove fault system.

As shown in Figure 6, the number of aftershocks with **M** > 3 within 24 hour periods following each mainshock were 121 (24 August), 75 (26 October), and 258 (30 October). The aftershocks following the three considered mainshocks have clear spatial patterns. For the 24 August event, most aftershock epicenters are not within the surface projection of the finite fault model, with many south and west of the rupture. This pattern holds for the 26 October event as well. The aftershocks pattern for the largest event (30 October) follows the expected pattern in which most epicenters occur within the surface projection of the rupture.

Table 2. Summary of the six main events that occurred in Central Italy between 24 August and 30 October 2016

Date	Hour (UTC)	Latitude (N)	Longitude (E)	Depth (km)	**M**	Strike (deg)	Dip (deg)
08/24/2016	**01:36:32**	**42.70**	**13.23**	**8**	**6.1**	**168**	**41**
						Mt. Vettore-Mt. Bove fault system	
						163	**52**
						Amatrice fault	
08/24/2016	02:33:28	42.79	13.15	8	5.3	134	56
08/26/2016	04:28:25	42.60	13.29	9	4.8	165	36
10/26/2016	17:10:36	42.88	13.13	9	5.4	160	38
10/26/2016	**19:18:05**	**42.92**	**13.13**	**8**	**5.9**	**158**	**43**
10/30/2016	**06:40:17**	**42.84**	**13.11**	**5**	**6.5**	**156**	**43**

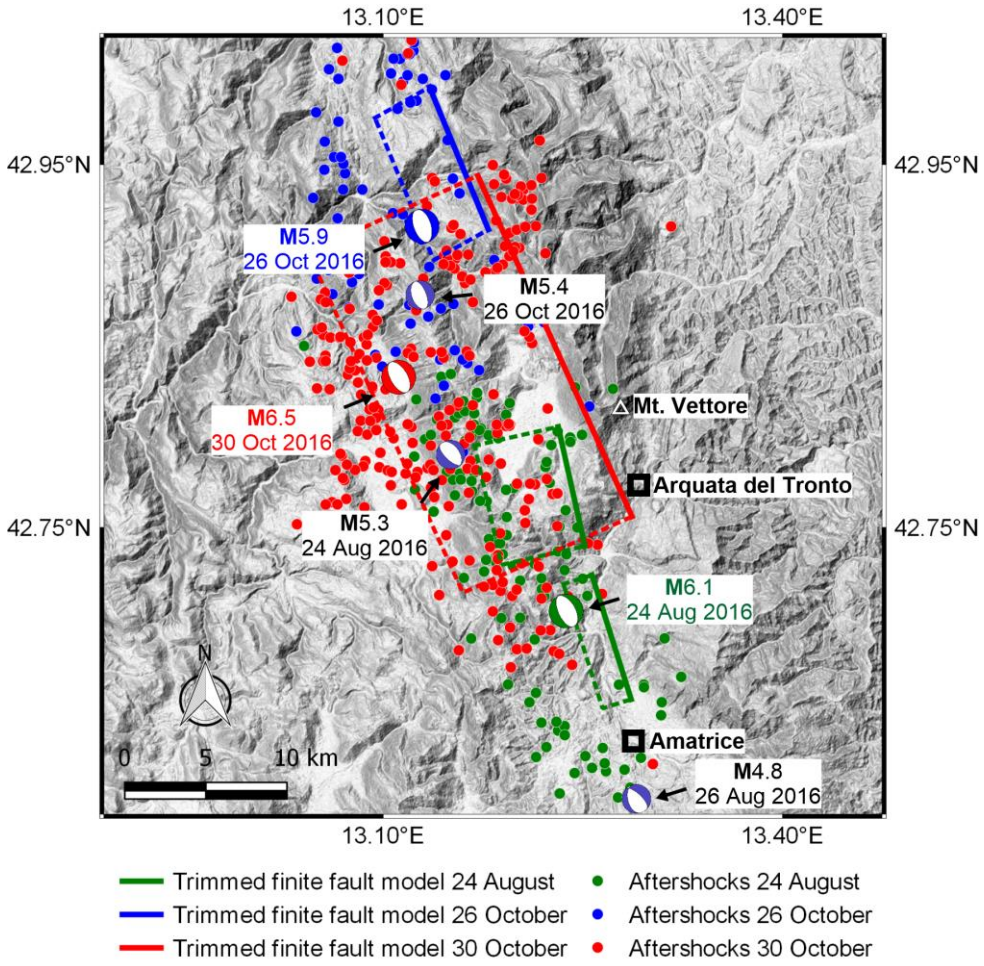

Figure 5. Map showing locations of hypocenters for three mainshock events in central Italy between 24 August and 30 October 2016. Also shown are selected finite fault models for each event and aftershock patterns for the 24-hour periods post-rupture.

FINITE FAULT MODELS

Finite fault models of the seismic source are needed for ground motion analysis, which typically uses distance metrics such as closest distance to rupture plane (R_{rup}) or closest distance to surface projection (R_{JB}). This section briefly reviews the data used in the inversions of finite fault models and the models themselves, including trimming of the rupture dimensions applied in the present work.

CONSIDERED DATA

In this section, we revisit the mechanisms of all three main shocks that occurred during the 2016-2017 Central Italy earthquake sequence (**M**6.1 24 August 2016, **M**5.9 26 October 2016, and **M**6.5 30 October 2016). We present a new source model that simultaneously fits the available measurements of the observed surface deformation. As in previous studies (Cheloni et al., 2017) for the 24 August **M**6.1 and 26 October **M**5.9 events, we use GPS data and

interferometric aperture radar (InSAR) measurements involving the ALOS-2 sensor. For the 30 October **M**6.5 event, we use the elastic dislocation modeling to determine the slip distribution of the causative fault, integrating GPS and InSAR measurements with static displacements derived from six strong motion stations. In this approach, static displacements from ground motion records are used to complement GPS and InSAR measurements. While both the GPS coseismic offsets and the ALOS-2 interferogram, relevant only to the 30 October earthquake have been already described in Cheloni et al. (2017), the static displacements derived from the closets stations have never been previously used in the source modeling and are presented here.

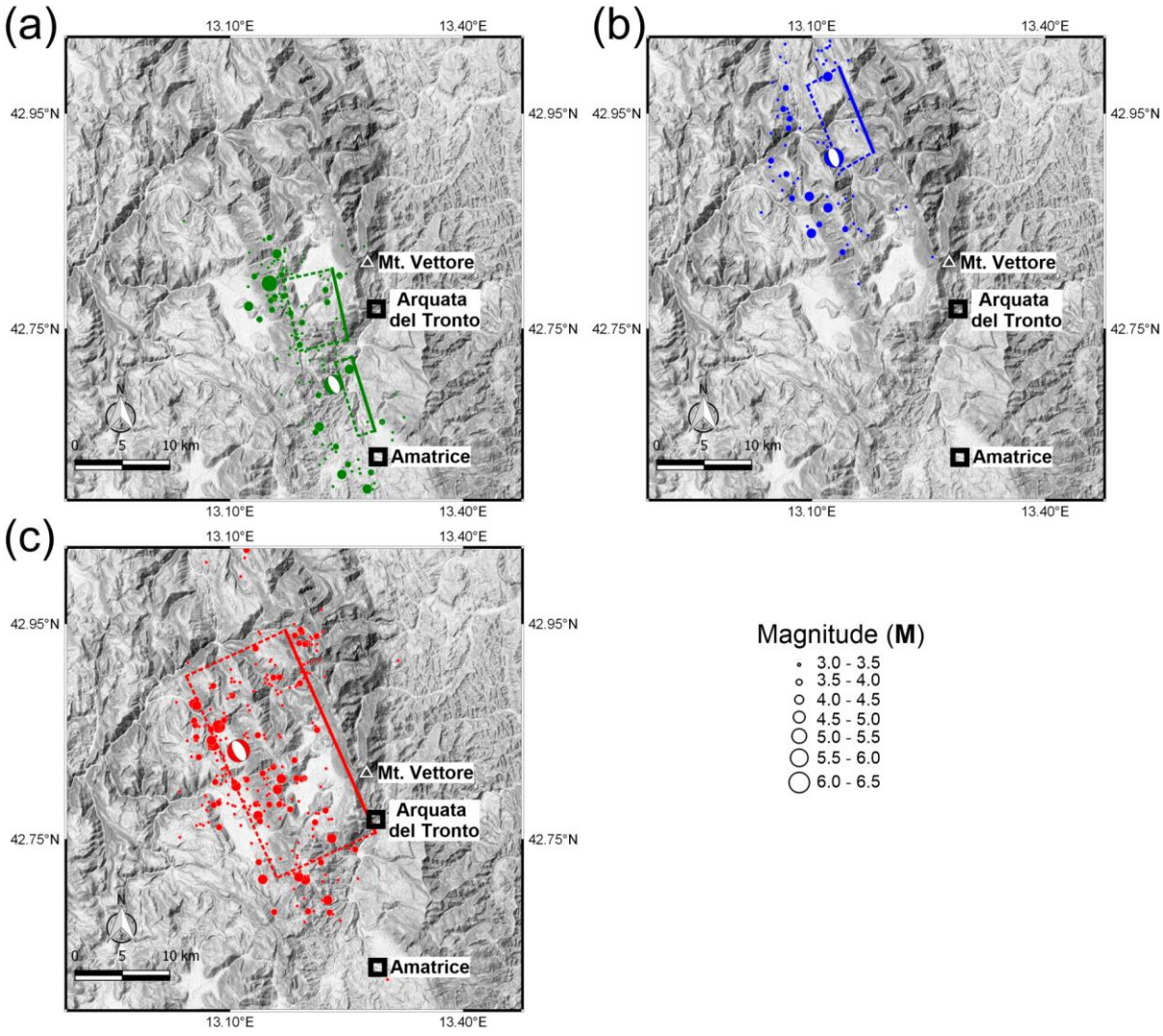

Figure 6. Spatial pattern of aftershocks that occurred in 24 hour periods following mainshocks on (a) 24 August, (b) 26 October, and (c) 30 October 2016. The finite fault model for each mainshock is added to the Figures (next section).

Near-fault strong motion data has been analyzed using special procedures (i.e. Gregor et al., 2002) for the following stations: (1) Amatrice (AMT), (2) Accumoli (ACC), (3) Castelluccio di Norcia (CLO), (4) Castelsantangelo sul Nera (CNE), (5) Forca Canapine (T1214), and (6) Castelvecchio (T1216). Those procedures preserve fling-step displacements (i.e. earthquake-related static ground displacements, resulting from fault rupture).

The largest static coseismic offsets identified from strong motion data (up to 50-80 cm) were observed in the Castelluccio plain, coinciding with the area of the maximum observed deformation as depicted by InSAR interferograms spanning the 30 October earthquake (Cheloni et al., 2017). As shown in Figure 7, data from the CLO station indicates horizontal offsets of about 52 cm towards the SW and about 87 cm of vertical subsidence. The CNE station indicates horizontal movement of about 22 cm towards the SW and subsidence of about 15 cm. Other strong motion stations (T1216, ACC, AMT, and T1214) are almost co-located with GPS stations and show horizontal and vertical coseismic displacements in agreement with the estimated GPS offsets (Figure 7). The CLO and CNE strong motion stations, do not have co-located GPS sensors. As a result, these stations provide additional displacement data useful for constraining the fault slip distribution for the **M**6.5 30 October event.

SELECTED MODELS

Cheloni et al. (2017) presents finite fault models for the 24 August and 26 and 30 October earthquakes. The trimmed versions of these models are shown in Figure 8. Details on the trimming procedure are given by GEER (2016). For the 30 October event, we performed new modeling using rectangular dislocations in a homogeneous elastic half-space (Okada, 1985) to infer the slip distribution responsible for the surface displacements, as described in Cheloni et al. (2014, 2016). In the modeling, we used a fault plane geometry (156°/43°, strike/dip) for the 30 October **M**6.5 Norcia earthquake that is taken from Cheloni et al. (2017) with a small translation and rotation to make it consistent with the new data set, and invert for the best-fitting displacements of the dislocations, solving for rake and slip magnitude on each fault patch. In addition, to better constrain the slip pattern in the inversion we also considered the hypothesis, based on geodetic data, that a certain amount of slip during the 30 October earthquake occurred on an antithetic fault (Figure 1c). To help fit the data better, we consider a scenario with further slip on a an antithetic normal fault in addition to the majority of the coseismic slip estimated on the Mt. Vettore-Mt. Bove fault related to the main shock. In

particular, we used the position and geometry of the antithetic fault (335°/50°, strike/dip) proposed by Cheloni et al. (2017) and well illuminated by aftershocks recorded three months following the earthquake (Chiaraluce et al. 2017).

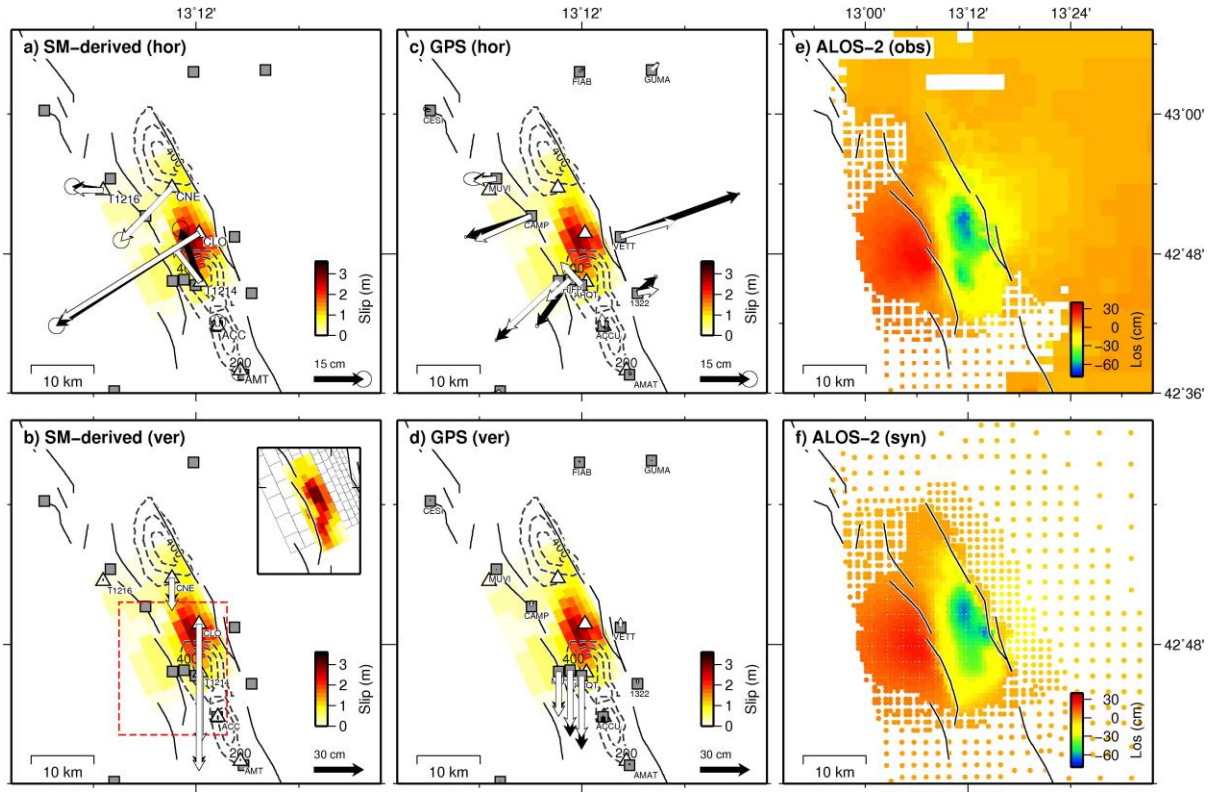

Figure 7. (a) Strong motion (SM)-derived (black) and predicted (white) horizontal and (b) vertical displacements, (c) observed (black) and predicted (white) GPS horizontal and (d) vertical displacements, (e) observed and (f) modeled displacement fields from the unwrapped ALOS-2 interferograms, relative to the **M**6.5 30 October event. The slip distributions are shown in panels a-d: the dashed lines are the contours of the 24 August and 26 October earthquakes from Cheloni et al. (2017), while the colors indicate an updated coseismic slip distribution of the 30 October event. The inset in panel (b) represent the modelled antithetic fault.

Our best-fit model can explain each data set reasonably well (RMS 2.6, 5.0 and 2.0 cm for GPS, InSAR and SM, respectively). The results show that the slip is concentrated in one main asperity within a depth of 0-7 km and the rupture touches the free surface in correspondence to the observed surface breaks (Gori et al., this issue) for a total length of > 15 km, in agreement with the results of Cheloni et al. (2017). It is worth noting that where field mapping studies (Civico et al., 2018; Villani et al., 2018; Gori et al., this issue) documented the maximum surface breaks (up to > 1.5 m), the estimated shallow coseismic slip also reaches the maximum values. Finally, our model indicates a seismic moment of 9.04 × 10^{18} Nm, equivalent to a **M**6.6 earthquake released by the Mt.Vettore-Mt. Bove fault system. The antithetic fault released a slip equivalent to an earthquake of magnitude 6.0.

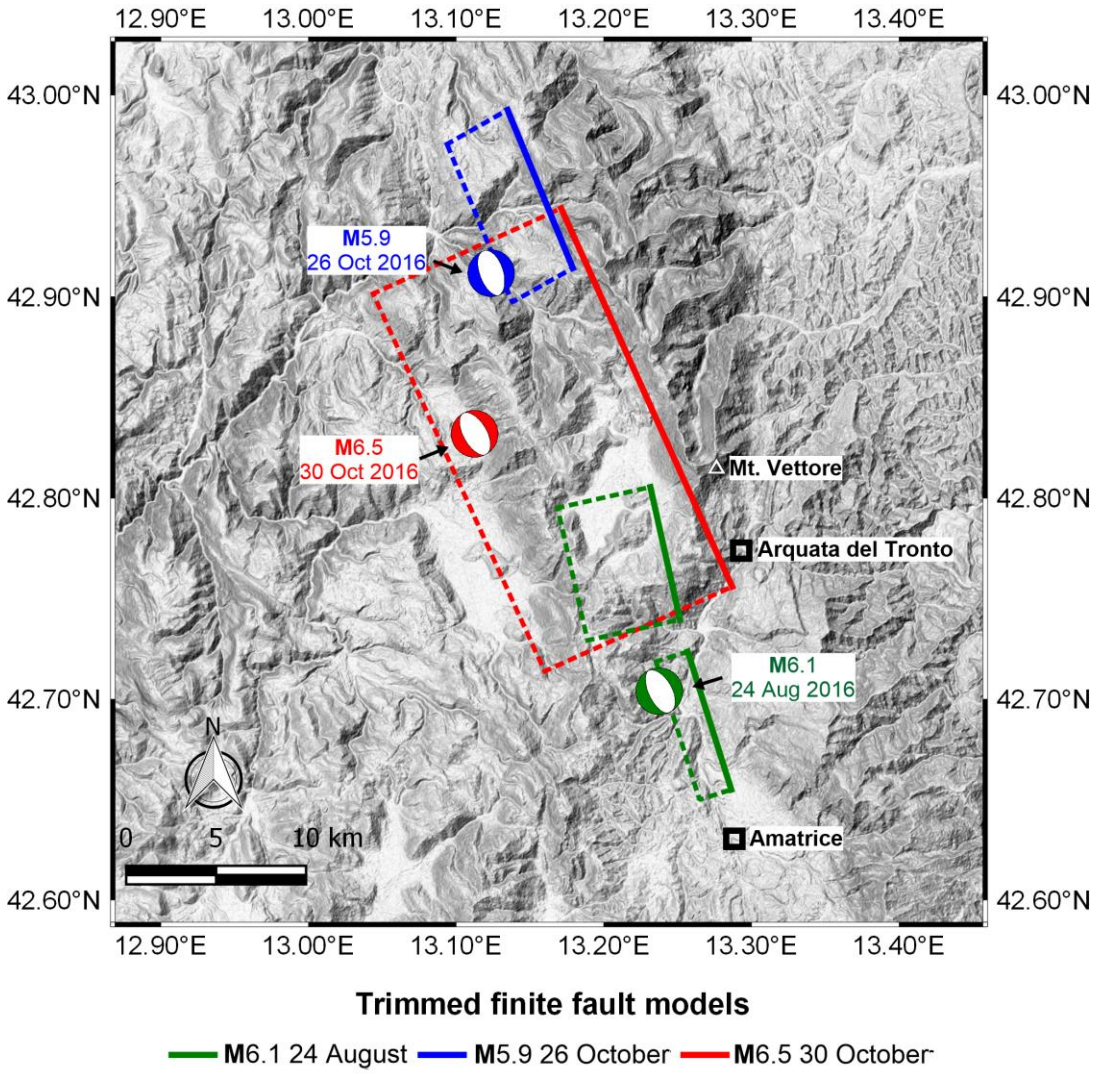

Figure 8. Surface projections of the trimmed finite fault models for the **M**6.1 24 August, **M**5.9 26 October, and **M**6.5 30 October events.

CONCLUSIONS

In this paper, we describe the Quaternary/active faulting setting for the region that produced the 2016-2017 Central Italy earthquake sequence, with an emphasis on the faults to which the mainshocks are attributed. We also present source attributes of the mainshocks (focal mechanisms and finite fault models) that support the conclusion that the causative fault for these events was principally the Mt. Vettore-Mt. Bove fault system with the Amatrice fault to the south being involved in the 24 August 2016 event.

In our analysis of regional fault systems and the present earthquake sequence, we address issues of fault segmentation based on Quaternary geological evidence, and the degree to which single earthquake events can rupture one or more seismogenic faults or multiple

adjacent segments of a single fault system. We review current understanding of this subject for regional faults based on fault geometry, paleoseismic studies, neotectonic analyses (concerning the evidence of fault activity through the Quaternary), and historical earthquake observations. Most of the faults in the region are considered unlikely to rupture with neighboring faults as multi-fault ruptures, due to kinematic differences expressed by different long term (Quaternary) activity, relatively large gaps between faults and different strike and dip angles, any of which suggest kinematically independent structures. Of course, the potential for rupture on one seismogenic source to dynamically trigger ruptures on nearby faults is present to varying degrees.

The Mt. Vettore-Mt. Bove fault system and the Amatrice fault are relatively proximate and share similar strike and dip angles. They are considered different fault systems because of the presence of the Ancona-Anzio lithospheric fault, representing a kinematic separation between them. Falcucci et al. (2018) show that the presence of this lithospheric structure allowed slip transfer between the two structures during the 24 August 2016 event. The observations from the initial mainshock in the sequence (24 August 2016) was that rupture involved both fault systems, which is relatively unusual for the region. The subsequent 30 October event produced rupture on multiple segments of the Mt. Vettore-Mt. Bove fault system. Hence, these events provide valuable data that give rise to more complex questions on how earthquake ruptures can cross between separate segments and faults in an extensional environment. A more nuanced discussion of this issue is provided by Lyakhovsky et al. (2016). We provide tabular information on the principal fault systems in the region, including earthquake size, recurrence and segment geometries. We anticipate that this collection of information will be useful in future source modeling studies. Moreover, we provide source attributes for the mainshock events in the 2016-2017 earthquake sequence, which will be useful for ground motion studies, including those presented in Zimmaro et al. (this 2018, in this issue).

ACKNOWLEDGMENTS

The authors acknowledge two anonymous Reviewer and the Reviewer Professor Silvio Seno whose criticisms and suggestions helped us to improve the overall quality of the paper. The GEER Association is supported by the National Science Foundation (NSF) through the Geotechnical Engineering Program under Grant No. CMMI-1266418. Any opinions, findings, and conclusions or recommendations expressed in this material are those of the

authors and do not necessarily reflect the views of the NSF. The GEER Association is made possible by the vision and support of the NSF Geotechnical Engineering Program Directors: Dr. Richard Fragaszy and the late Dr. Cliff Astill. GEER members also donate their time, talent, and resources to collect time-sensitive field observations of the effects of extreme events. We thank Giuseppe Tropeano at University of Cagliari for proving technical support on the analysis of strong motion data.

REFERENCES

Akinci, A., Galadini, F., Pantosti, D., Petersen, M.D., Malagnini, L., and Perkins, D.M., 2009. Effect of the time-dependence on probabilistic seismic hazard maps and deaggregation for the central Apennines, Italy, *Bull. Seismol. Soc. Am.* **99**, 585-610.

Barchi, M.R., and Mirabella, F., 2009. The 1997–98 Umbria–Marche earthquake sequence: "Geological" vs."seismological" faults, *Tectonophysics* **476**, 170-179.

Boncio, P., Lavecchia, G., and Pace, B., 2004a. Defining a model of 3D seismogenic sources for Seismic Hazard Assessment applications: the case of central Apennines (Italy), *J. Seism.* **8**, 407–425.

Boncio, P., Lavecchia, G., Milana, G., and Rozzi, B., 2004b. Improving the knowledge on the seismogenesis of the Amatrice-Campotosto area (central Italy) through an integrated analysis of minor earthquake sequences and structural data, *Ann. Geophys.* **47**, 1723–1742.

Bonini, L., Maesano, F. E., Basili, R., Burrato, P., Carafa, M. M. C., Fracassi, U., et al., 2016. Imaging the tectonic framework of the 24 August 2016, Amatrice (central Italy) earthquake sequence: New roles for old players? *Annals of Geophysics* **59**, Fast Track 5, DOI: https://doi.org/ 10.4401/ag-7229

Cacciuni, A., Centamore, E., Di Stefano, R., and Dramis, F., 1995. Evoluzione morfotettonica della conca di Amatrice, *Studi Geol. Camerti* **2**, 95–100.

Calamita, F., and Pizzi, A., 1992. Tettonica quaternaria nella dorsale appenninica umbro-marchigiana e bacini intrappenninici associati, *Studi Geologici Camerti* **1**, 17-25.

Calamita, F., Coltorti, M., Piccinini, D., Pierantoni, P. P. Pizzi, A., Ripepe, M., Scisciani, and V., Turco, E., 2000. Quaternary faults and seismicity in the Umbro-Marchean Apennines (central Italy). *Journal of Geodynamics*, **29** 245-264.

Calamita, F., Pizzi, A., Scisciani, V., De Girolamo, C., Coltorti, M., Pieruccini, P., and Turco, E., 2000. Caratterizzazione delle faglie quaternarie nella dorsale appenninica umbro-marchigiano-abruzzese. In F. Galadini, C. Meletti, & A. Rebez (Eds.), Le Ricerche del GNDT nel campo della

pericolosità simica (1996-1999), (p. 397). Roma: CNR-Gruppo Nazionale per la Difesa dai Terremoti.

Carminati, E., and Doglioni, C., 2012. Alps vs. Apennines: The paradigm of a tectonically asymmetric Earth, *Earth-Science Reviews* **112**, 67–96.

Castelli, V., Camassi, R., Caracciolo, C.H., Locati, M., Meletti, C., and Rovida, A., 2016. New insights in the seismic history of Monti della Laga area, *Annals of Geophysics* **59**, Fast Track 5, 2016; doi: 10.4401/ag-7243.

Castelli, V., Galadini, F., Galli, P., Molin, D., and Stucchi, M., 2002. Caratteristiche sismogenetiche della sorgente della Laga e relazione con il terremoto del 1639. In ProcEedings, 21st meeting of Gruppo Nazionale di Geofisica della Terra Solida, Rome, Italy.

Cavinato, G. P., and De Celles, P., 1999. Extensional basins in the tectonically bimodal central Apennines fold-thrust belt, Italy: Response to corner flow above a subducting slab in retrograde motion, *Geology* **27**, 955-958.

Cavinato, G.P., Cosentino D., De Rita D., Funiciello R., Parotto M., 1994. Tectonic-sedimentary evolution of intrapenninic basins and correlation with the volcano-tectonic activity in central Italy. *Mem. Descr. Carta Geol. d'It.*, **49**, 63-76.

Cello, G., Deiana, G., Ferelli, L., Marchegiani, L., Maschio, L., Mazzoli, S., Michetti, A., Serva, L., Tondi, E., and Vittori, T., 2000. Geological constraints for earthquake faulting studies in the Colfiorito area (central Italy), *J. Seism.*, **4**, 357-364.

Cello, G., Mazzoli, S., Tondi, E., and Turco, E., 1997. Active tectonics in the Central Apennines and possible implications for seismic hazard analysis in peninsular Italy, *Tectonophysics* **272**, 43-68.

Centamore, E. and Rossi, D., 2009. Neogene-Quaternary tectonics and sedimentation in the Central Apennines. *Ital.J.Geosci. (Boll.Soc.Geol.It.)* **128**, 73-88,

Cheloni, D., De Novellis, V., Albano, M., Antonioli, A., Anzidei, M., Atzori, S., Avallone, A., Bignami, C., Bonano, M., Calcaterra, S., Castaldo, R., Casu, F., Cecere, G., De Luca, C., Devoti, R., Di Bucci, D., Esposito, A., Galvani, A., Gambino, P., Giuliani, R., Lanari, R., Manunta, M., Manzo, M., Mattone, M., Montuori, A., Pepe, A., Pepe, S., Pezzo, G., Petrantonio, G., Polcari, M., Riguzzi, F., Salvi, S., Sepe, V., Serpelloni, E., Solaro, G., Stramondo S., Tizzani, P., Tolomei, C., Trasatti, E., Valerio E., Zinno, I., and Doglioni, C., 2017. Geodetic model of the 2016 Central Italy earthquake sequence inferred from InSAR and GPS data, *Geophysical Research Letters* **44**, 6778-6787.

Cheloni, D., Giuliani, R., D'Anastasio, E., Atzori, S., Walters, R. J., Bonci, L., D'Agostino, N., Mattone, M., Calcaterra, S., Gambino, P., Deninno, F., Maseroli, R., and Stefanelli, G., 2014.

Coseismic and post-seismic slip of the 2009 L'Aquila (central Italy) Mw 6.3 earthquake and implications for seismic potential along the Campotosto Fault from joint inversion of high-precision levelling, InSAR and GPS data, *Tectonophysics* **622**, 168-185.

Cheloni, D., Serpelloni, E., Devoti, R., D'Agostino, N., Pietrantonio, G., Riguzzi, F., Anzidei, M., Avallone, A., Cavaliere, A., Cecere, G., D'Ambrosio, C., Esposito, A., Falco, L., Galvani, A., Selvaggi, G., Sepe, V., Calcaterra, S., Giuliani, R., Mattone, M., Gambino, P., Abruzzese, L., Cardinale, V., Castagnozzi, A., De Luca, G., Massucci, A., Memmolo, A., Migliari, F., Minichiello, F., and Zarrilli, L., 2016. GPS observations of coseismic deformation following the 2016, August 24, Mw 6 Amatrice earthquake (central Italy): data, analysis and preliminary fault model, *Annals of Geophysics* **59**, Fast Track 5, 2016; doi: 10.4401/ag-7269.

Chiarabba, C., Amato, A., Anselmi, M., Baccheschi, P., Bianchi, I., Cattaneo, M., Cecere, G., Chiaraluce, L., Ciaccio, M. G., De Gori, P., De Luca, G., Di Bona, M., Di Stefano, R., Faenza, L., Govoni, A., Improta, L., Lucente, F. P., Marchetti, A., Margheriti, L., Mele, F., Michelini, A., Monachesi, G., Moretti, M., Pastori, M., Piana Agostinetti, N., Piccinini, D., Roselli, P., Seccia, D., and Valoroso, L., 2009. The 2009 L'Aquila (central Italy) Mw 6.3 earthquake: main shock and aftershocks, *Geophys. Res. Lett.* **36**, 1–6.

Chiaraluce, L., 2012. Unravelling the complexity of Apenninic extensional fault systems: A review of the 2009 L'Aquila earthquake (Central Apennines, Italy), *Journal of Structural Geology* **42**, 2-18.

Chiaraluce, L., Barchi, M., Collettini, C., Mirabella, F., and Pucci, S., 2005. Connecting seismically active normal faults with Quaternary geological structures in a complex extensional environment: The Colfiorito 1997 case history (northern Apennines, Italy), *Tectonics* TC1002, doi:10.1029/2004TC001627.

Chiaraluce, L., Di Stefano, R., Tinti, E., Scognamiglio, L., Michele, M., Casarotti, E., Cattaneo, M., De Gori, P., Chiarabba, C., Monachesi, G., Lombardi, A., Valoroso, L., Latorre, D., and Marzorati, S., 2017. The 2016 Central Italy seismic sequence: a first look at the mainshocks, aftershocks, and source models, *Seism. Res. Lett.* **88**, 757-771.

Ciarapica, G., and Passeri, L., 1998. Evoluzione paleogeografica degli Appennini, *Atti Tic. Sc. Terra* **40**, 233-290.

Cipollari, P., Cosentino, D., Esu, D., Girotti, O., Gliozzi, E., Praturlon, A., 1999. Thrust-top lacustrine-lagoonal basin development in accretionary wedges: late Messinian (Lago- Mare) episode in the central Apennines (Italy), *Palaeogeogr., Palaeoclimatol., Palaeoecol.* **151**, 146-166.

669 Civico, R., Pucci, S., Villani, F., Pizzimenti, L., De Martini, P. M., Nappi, R.,and the Open
670 EMERGEO Working Group, 2018. Surface ruptures following the 30 October 2016 Mw 6.5
671 Norcia earthquake, central Italy. *Journal of Maps*.
672 https://doi.org/10.1080/17445647.2018.1441756

673 Coltorti, M., and Farabollini, P., 1995. Quaternary evolution of the Castelluccio di Norcia Basin, *Il*
674 *Quaternario* **8**, 149-166.

675 Cosentino, D., Asti, R., Nocentini, M., Gliozzi, E., Kotsakis, T., Mattei, M., Esu, D., Spadi, M.,
676 Tallini, M., Cifelli, F., Pennacchioni, M., Cavuoto, G. and Di Fiore, V., 2017. New insights into
677 the onset and evolution of the central Apennine extensional intermontane basins based on the
678 tectonically active L'Aquila Basin (central Italy), *Geological Society of America Bulletin* **129**,
679 1314-1336.

680 Cosentino, D., Cipollari, P., Marsili, P., and Scrocca, D., 2010. The Geology of Italy, 2010. *Journal of*
681 *the Virtual Explorer*, **36**, paper 11.

682 D'Agostino, N., Mantenuto, S. D'Anastasio, E. Giuliani, R. Mattone, M. Calcaterra, S. Gambino,
683 P., and Bonci, L., 2011. Evidence for localized active extension in the central Apennines (Italy)
684 from global positioning system observations, *Geology* **39**, 291-294.

685 D'Agostino, N., Jackson, J. A., Dramis, F., and Funiciello, R., 2001. Interactions between mantle
686 upwelling, drainage evolution and active normal faulting: an example from the central Apennines
687 (Italy), *Geophys. J. Int.* **147**, 475–479.

688 Devoti, R., D'Agostino, N., Serpelloni, E., Pietrantonio, G., Riguzzi, F., Avallone, A., Cavaliere, A.,
689 Cheloni, D., Cecere, G., D'Ambrosio, C., Franco, L., Selvaggi, G., Metois, M. Esposito, A., Sepe,
690 V., Galvani, A., and Anzidei, M., 2017. A Combined Velocity Field of the Mediterranean Region,
691 *Annals of Geophysics* **60**, S0215, doi:10.4401/ag-7059.

692 Devoti, R., Esposito, A., Pietrantonio, G., Pisani, A. R., and Riguzzi, F., 2011. Evidence of large scale
693 deformation patterns from GPS data in the Italian subduction boundary, *Earth Planet. Sci. Lett.*
694 **311**, 230-241.

695 Di Domenica, A., Petricca, P., Trippetta, F., Carminati, E. and Calamita, F., 2014. Investigating fault
696 reactivation during multiple tectonic inversions through mechanical and numerical modeling: An
697 application to the central-northern Apennines of Italy, *Journal of Structural Geology* **67**, 167–
698 185.

699 DISS Working Group, 2015. Database of Individual Seismogenic Sources (DISS), Version 3.2.0: A
700 compilation of potential sources for earthquakes larger than M 5.5 in Italy and surrounding areas.

Istituto Nazionale di Geofisica e Vulcanologia, available at: http://diss.rm.ingv.it/diss/, last accessed 12 October 2017, doi: 10.6092/INGV.IT-DISS3.2.0.

EMERGEO Working Group, 2016. Coseismic effects of the 2016 Amatrice seismic sequence: First geological results, *Annals of Geophysics* **59**, Fast Track 5, doi: https://doi.org/10.4401/ag-7195.

Falcucci, E., Gori, S., Bignami, C., Pietrantonio, G., Melini, D., Moro, M., Saroli, M. and Galadini, F., 2018. The Campotosto seismic gap in between the 2009 and 2016–2017 seismic sequences of central Italy and the role of inherited lithospheric faults in regional seismotectonic settings, *Tectonics* **37**. https://doi.org/10.1029/2017TC004844

Falcucci, E., Gori, S., Galadini, F., Fubelli, G., Moro, M., and Saroli, M., 2016. Active faults in the epi-central and mesoseismal Ml 6.0 24, 2016 Amatrice earthquake region, central Italy. Methodological and seismotectonic issues, *Annals of Geophysics* **59**, Fast Track 5, 2016. DOI: 10.4401/ ag-7266.

Falcucci, E., Gori, S., Moro, M., Fubelli, G., Saroli, M., Chiarabba, C. and Galadini, F., 2015. Deep reaching versus vertically restricted Quaternary normal faults: implications on seismic potential assessment in tectonically active regions. Lessons from the middle Aterno valley fault system, central Italy, Tectonophysics **305**, 350-358.

Ferrarini, F., Lavecchia, G., de Nardis, R., and Brozzetti, F., 2015. Fault geometry and active stress from earthquakes and field geology data analysis: the Colfiorito 1997 and L'Aquila 2009 Cases (Central Italy), *Pure and Applied Geophysics* **172**, 1079-1103.

Fubelli, G., Gori, S., Falcucci, E., Galadini, F., and Messina, P., 2009. Geomorphic signatures of recent normal fault activity versus geological evidence of inactivity: Case studies from the central Apennines (Italy), *Tectonophysics* **476**, 252-268.

Galadini, F., and Galli, P., 1999. The Holocene paleoearthquakes on the 1915 Avezzano earthquake faults (central Italy): implications for active tectonics in Central Apennines, *Tectonophysics* **308**, 143-170.

Galadini, F., and Galli, P., 2000. Active tectonics in the Central Apennines (Italy) - Input data for seismic hazard Assessment, *Natural Hazards* **22**, 225-270.

Galadini, F., and Galli, P., 2000. Active tectonics in the Central Apennines (Italy) - Input data for seismic hazard Assessment, *Natural Hazards* **22**, 225-270.

Galadini, F., and Galli, P., 2003. Paleoseismology of silent faults in the Central Apennines (Italy): the Mt. Vettore and Laga Mts. Faults, *Annals of Geophysics* **46**, 815-836.

Galadini, F., and Messina, P., 2001. Plio-Quaternary changes of the normal fault architecture in the central Apennines (Italy), *Geodinamica Acta* **14**, 321-344.

Galadini, F., and Messina, P., 2004. Early–Middle Pleistocene eastward migration of the Abruzzi Apennine (central Italy) extensional domain, *Journal of Geodynamics* **37**, 57-81.

Galadini, F., Falcucci E., Galli P., Giaccio B., Gori S., Messina P., Moro M., Saroli M., Scardia G., and Sposato A., 2012. Time intervals to assess active and capable faults for engineering practices in Italy, *Engineering Geology* **139/140**, 50-65.

Galadini, F., Messina, P., Giaccio, B., and Sposato, A., 2003. Early uplift history of the Abruzzi Apennines (central Italy): available geomorphological constraints, *Quat. Int.* **101/102**, 125-135.

Galadini. F., Galli, P., Leschiutta, I., Monachesi, G., and Stucchi, M., 1999. Active tectonics and seismicity in the area of the 1997 earthquake sequence in central Italy: a short review, *Journal of Seismology* **3**, 167-175.

Galli, P., Galadini, F., and Calzoni, F., 2005. Surface faulting in Norcia (central Italy): a "paleoseismological perspective", *Tectonophysics* **403**, 117-130.

Galli, P., Galadini, F., and Pantosti, D., 2008. Twenty years of paleoseismology in Italy, *Earth Science Reviews* **88**, 89–117.

GEER, 2016. *Engineering Reconnaissance of the 24 August 2016 Central Italy Earthquake. Version 2*, Zimmaro P. and Stewart J.P. (editors), Geotechnical Extreme Events Reconnaissance Association Report No. GEER-050B. doi: 10.18118/G61S3Z.

GEER, 2017. *Engineering Reconnaissance following the October 2016 Central Italy Earthquakes - Version 2*, Zimmaro P. and Stewart J.P. (editors), Geotechnical Extreme Events Reconnaissance Association Report No. GEER-050D. doi:10.18118/G6HS39.

Gori, S., Falcucci, E., Galadini, F., Zimmaro, P., Stewart, J. P., Kayen R. E., Lingwall, B., Moro, M., Saroli, M., Pizzi, A., and Di Domenica, A. 201x. Surface faulting caused by the 2016 Central Italy seismic sequence, *Earthquake Spectra*, In review.

Gruppo di Lavoro sul terremoto di Visso, 2016. *Rapporto di sintesi sul Terremoto di Visso Ml 5.9 del 26 ottobre 2016 (Italia Centrale)*, doi: 10.5281/zenodo.163818 (in Italian).

Huang, M.-H., Fielding, E. J., Liang, C., Milillo, P., Bekaert, D., Dreger, D. and Salzer J., 2017. Coseismic deformation and triggered landslides of the 2016 Mw 6.2 Amatrice earthquake in Italy. *Geophys. Res. Lett.*, **44**, 1266–1274, doi:10.1002/2016GL071687.

Lavecchia, G., Castaldo, R., de Nardis, R., De Novellis, V., Ferrarini, F., Pepe, S., Brozzetti, F., Solaro, G., Cirillo, D., Bonano, M., Boncio, P., Casu, F., De Luca, C., Lanari, R., Manunta, M.,

764 Manzo, M., Pepe, A., Zinno, I., and Tizzani, P., 2016. Ground deformation and source geometry
765 of the 24 August 2016 Amatrice earthquake (Central Italy) investigated through analytical and
766 numerical modeling of DInSAR measurements and structural-geological data, *Geophys. Res. Lett.*
767 **43**, DOI:10.1002/2016GL071723

768 Lyakhovsky, V., Ben-Zion, Y., Ilchev, A., and Mendecki, A., 2016. Dynamic rupture in a damage-
769 breakage rheology model, *Geophys. J. Int.* **206**, 1126-1134.

770 Malinverno, A. and Ryan, W. B. F., 1986. Extension in the Tyrrhenian sea and shortening in the
771 Apennines as result of arc migration driven by sinking of the lithosphere, Tectonics **5**, 227-245.

772 Messina, P., Galadini, F., Galli, P., and Sposato, A., 2002. Quaternary basin evolution and present
773 tectonic regime in the area of the 1997-98 Umbria-Marche seismic sequence (central Italy),
774 *Geomorphology* **42**, 97-116.

775 Michetti, A. M., Brunamonte, F., Serva, L., and Vittori, E., 1996. Trench investigations of the 1915
776 Fucino earthquake fault scarps (Abruzzo, Central Italy): geological evidence of large historical
777 events, *J. Geophys. Res.* **101**, 5921-5936.

778 Montone, P., and Mariucci, M. T., 2016. The new release of the Italian contemporary stress map,
779 *Geophysical Journal International* **205**, 1525-1531.

780 Moro, M., Bosi, V., Galadini, F., Galli, P., Giaccio, B., Messina, P., and Sposato, A., 2002. Analisi
781 paleosismologiche lungo la faglia del M. Marine (alta valle dell'Aterno): risultati preliminari, *Il*
782 *Quaternario* **15**, 267-278.

783 Pantosti, D., De Martini, P.M., Galli, P., Galadini, F., Messina, P., Moro, M., and Sposato, A. 1999.
784 Studi paleosismologici attraverso la rottura superficiale prodotta dal terremoto del 14 ottobre
785 1997 (Umbria-Marche). In Proceedings, 18th National Congress, November, 9-11, Rome, Italy..

786 Patacca, E., Scandone, P., Di Luzio, E., Cavinato, G. P., and Parotto M., 2008. Structural architecture
787 of the central Apennines: interpretation of the CROP 11 seismic profile from the Adriatic coast to
788 the orographic divide, *Tectonics* **27**, TC3006.

789 Pizzi, A., and Galadini, F., 2009. Pre-existing cross-structures and active fault segmentation in the
790 northern-central Apennines (Italy), *Tectonophysics* **476**, 304-319.

791 Pizzi, A., Calamita, F., Coltorti, M., and Pieruccini, P., 2002. Quaternary normal faults, intramontane
792 basins and seismicity in the Umbria-Marche- Abruzzi Apennine ridge (Italy): contribution of
793 neotectonic analysis to seismic hazard assessment, *Boll. Soc. Geol. It., Spec. Publ.* **1**, 923-929.

Porreca, M., Minelli, G., Ercoli, M., Brobia, A., Mancinelli, P., Cruciani, F., et al. 2018. Seismic reflection profiles and subsurface geology of the area interested by the 2016–2017 earthquake sequence (Central Italy), *Tectonics* **37**, 1116–1137. https://doi. org/10.1002/2017TC004915

Principi, P., 1911. Idrologia sotterranea della pianura di Norcia. Tipografia della Pace E. Cuggiani, Via della Pace 35, Roma.

Roberts, G. P., and Michetti, A. M., 2004. Spatial and temporal variations in growth rates along active normal fault systems: an example from the Lazio-Abruzzo Apennines, central Italy, *J. Struct. Geol.* **26**, 339-376.

Scisciani, V., Tavarnelli, E., and Calamita, F., 2002. The interaction of extensional and contractional deformations in the outer zones of the central Apennines, Italy, *Journal of Structural Geology* **24**, 1647-1658.

Scognamiglio, L., Tinti, E., Casarotti, E., Pucci, S., Villani, F., Cocco, M., et al., 2018. Complex fault geometry and rupture dynamics of the Mw 6.5, 2016, October 30th central Italy earthquake, *Journal of Geophysical Research: Solid Earth* **123**, 2943–2964.

Smeraglia, L., Billi, A., Carminati, E., Cavallo, A. and Doglioni, C., 2017. Field- to nano-scale evidence for weakening mechanisms along the fault of the 2016 Amatrice and Norcia earthquakes, Italy, *Tectonophysics* **712-713**, 156–169.

Storti, F., Balsamo F. and Koopman, A., 2017. Geological map of the partially dolomitized Jurassic succession exposed in the core of the Montagna dei Fiori Anticline, Central Apennines, Italy, *Italian Journal of Geosciences* **136**, 125-135.

Storti, F., Balsamo, F., Koopman, A., Mozafari, M., Solum, J., Swennen, R., and Taberne, C., 2016. Superimposed positive and negative inversion of the syn-rift fault network preserved in the Montagna dei Fiori Anticline, Central Apennines, Italy. In Proceedings, EGU General Assembly, 17-22 April, EGU2016-3057, Vienna, Austria..

Tinti, E., Scognamiglio, L., Michelini, A., and Cocco.M., 2016. Slip heterogeneity and directivity of the ML 6.0, 2016, Amatrice earthquake estimated with rapid finite-fault inversion, *Geophysical Research Letters* **43**, 10,745–10,752.

Tondi, E., 2000. Geological analysis and seismic hazard in the Central Apennines (Italy), *Journal of Geodynamics* **29**, 517-533.

Valoroso, L., Chiaraluce, L., Piccinini, D., Di Stefano, R., Schaff, D., and Waldhauser, F., 2013. Radiography of a normal fault system by 64,000 high-precision earthquake locations: The 2009 L'Aquila (central Italy) case study, *Journal of Geophysical Research: Solid Earth* **118**, 1156-1176.

827 Villani, F., Civico, R., Pucci, S., Pizzimenti, L., Nappi, R., De Martini, P. M., & the Open
828 EMERGEO Working Group, 2018. A database of the post-30 October 2016 Norcia earthquake
829 coseismic effects in central Italy. Scientific Data. https://doi.org/10.1038/sdata.2018.49

830 Vittori, E., Deiana, G., Esposito, E., Ferreli, L., Marchegiani, L., Mastrolorenzo, G., Michetti, A.M.,
831 Porfido, S., Serva, L., Simonelli, A.L., and Tondi, E., 2000. Ground effects and surface faulting in
832 the September–October 1997 Umbria–Marche (Central Italy) seismic sequence, *Journal of*
833 *Geodynamics* **29**, 535-564.

834 Ward, S.N., and Valensise, G., 1989. Fault parameters and slip distribution of the 1915 Avezzano,
835 Italy, earthquake derived from geodetic observations, *Bull. Seismol. Soc. Am.*, **79**, 690-710

836 Wooddell, K. E., and Abrahamson, N. A., 2014. Classification of main shocks and aftershocks in the
837 NGA-West2 database. *Earthquake Spectra*, **30**, 1257-1267.

838 Zimmaro, P., Scasserra, G., Stewart J. P., Kishida, T., Tropeano, G., Castiglia, M., and Pelekis, P.,
839 2018. Strong ground motion characteristics from 2016 Central Italy earthquake sequence,
840 *Earthquake Spectra*. DOI: 10.1193/091817EQS184M.

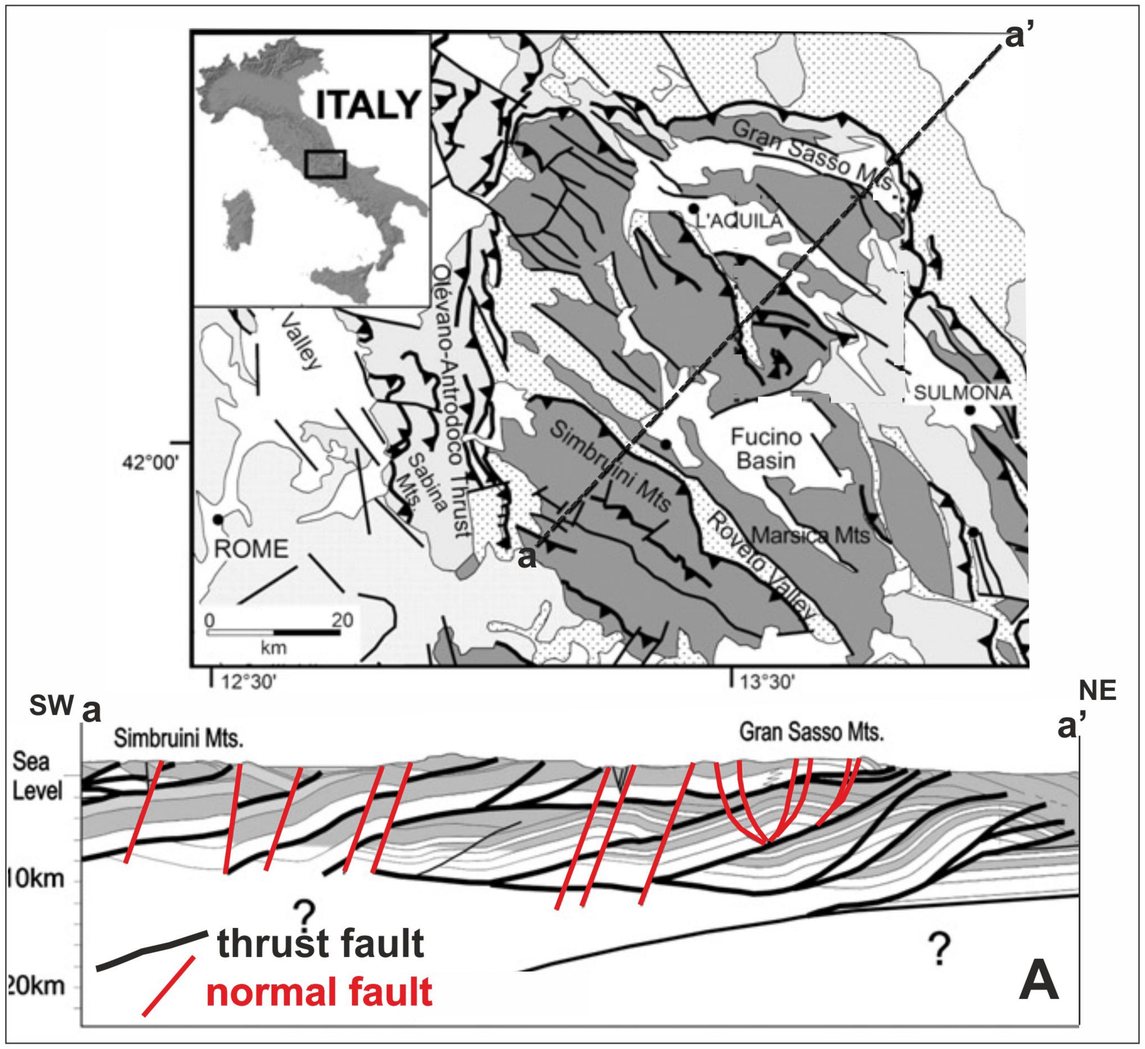
ITALY
a'
Gran Sasso Mts.
L'AQUILA
Olevano-Antrodoco Thrust
Valley
SULMONA
Fucino Basin
Simbruini Mts
Sabina Mts.
Roveto Valley
Marsica Mts
42°00'
ROME
a
0
20
km
12°30'
13°30'
SW
a
NE
a'
Simbruini Mts.
Gran Sasso Mts.
Sea Level
10km
20km
?
?
thrust fault
normal fault
A

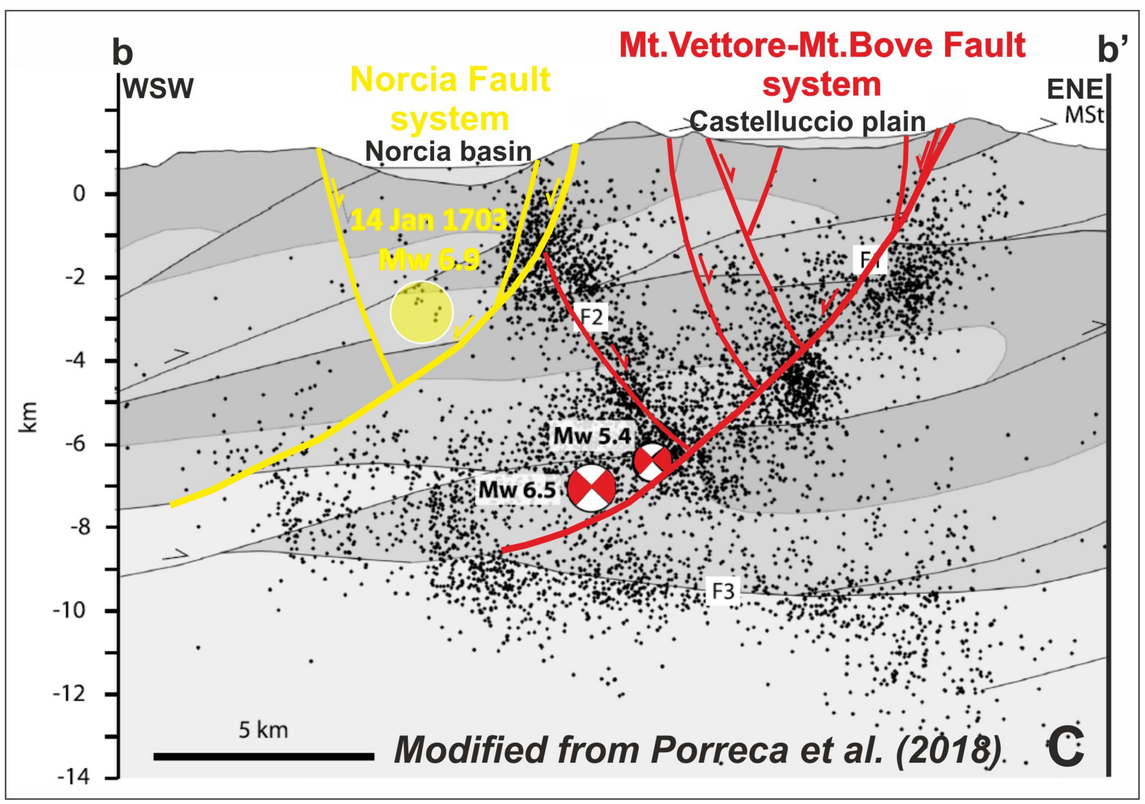
b
WSW
b'
ENE
MSt
Norcia Fault system
Norcia basin
Mt.Vettore-Mt.Bove Fault system
Castelluccio plain
14 Jan 1703
Mw 6.9
F1
F2
F3
Mw 5.4
Mw 6.5
0
-2
-4
-6
-8
-10
-12
-14
km
5 km
Modified from Porreca et al. (2018).
C

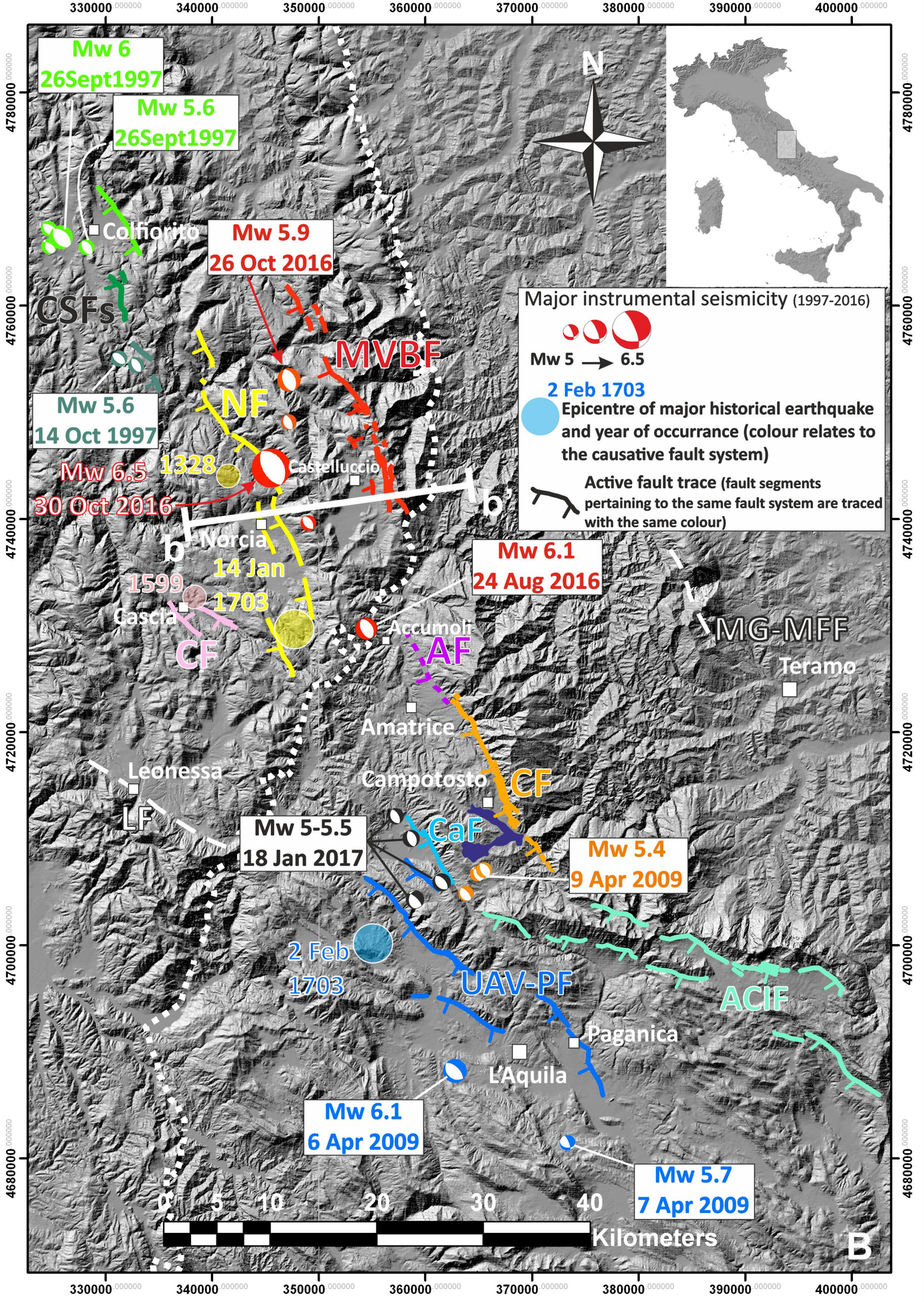
330000
340000
350000
360000
370000
380000
390000
400000
4780000
4760000
4740000
4720000
4700000
4680000
Mw 6
26Sept1997
Mw 5.6
26Sept1997
N
Colfiorito
Mw 5.9
26 Oct 2016
CSFs
MVBF
NF
Mw 5.6
14 Oct 1997
Mw 6.5
30 Oct 2016
1328
Castelluccio
b
b'
Norcia
14 Jan
1703
1599
Cascia
CF
Accumoli
AF
Mw 6.1
24 Aug 2016
MG-MFF
Teramo
Amatrice
Leonessa
LF
Campotosto
CF
CaF
Mw 5-5.5
18 Jan 2017
Mw 5.4
9 Apr 2009
2 Feb
1703
UAV-PF
ACIF
Paganica
L'Aquila
Mw 6.1
6 Apr 2009
Mw 5.7
7 Apr 2009
0
5
10
20
30
40
Kilometers
B
Major instrumental seismicity (1997-2016)
Mw 5
6.5
2 Feb 1703
Epicentre of major historical earthquake and year of occurrance (colour relates to the causative fault system)
Active fault trace (fault segments pertaining to the same fault system are traced with the same colour)


A

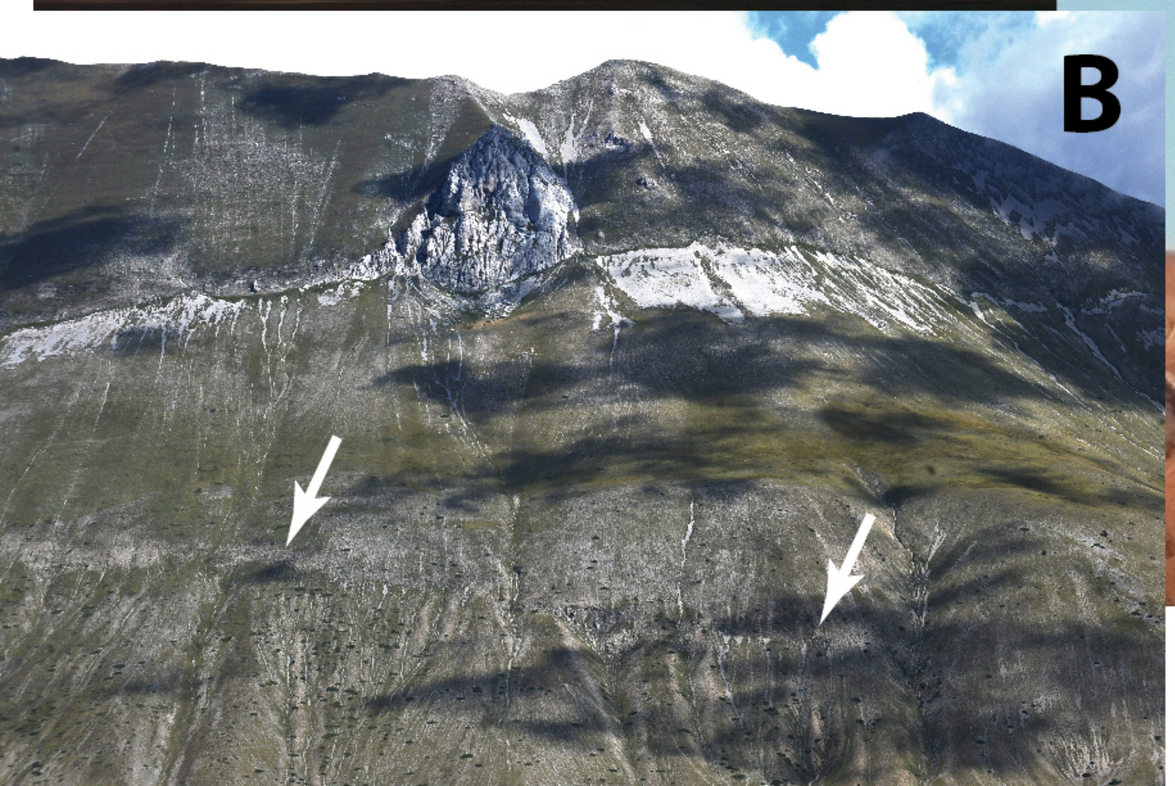
B

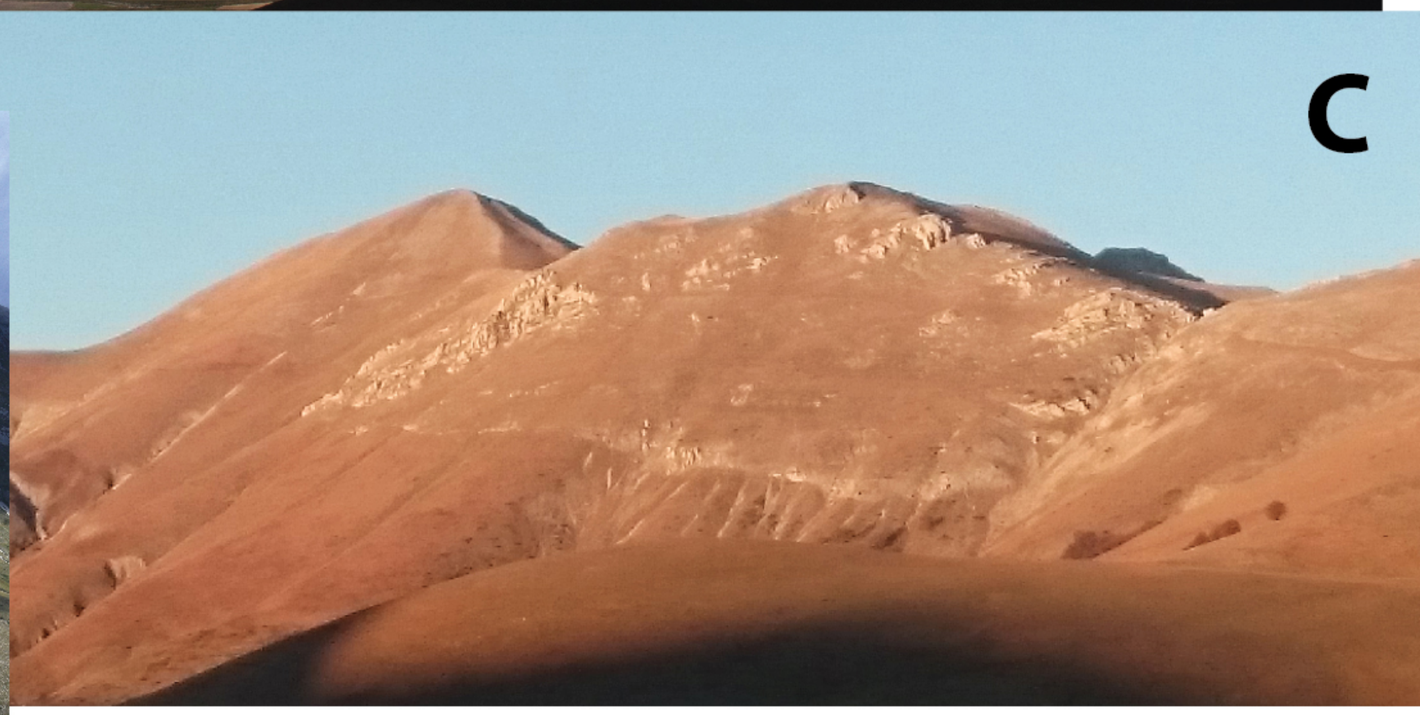
C

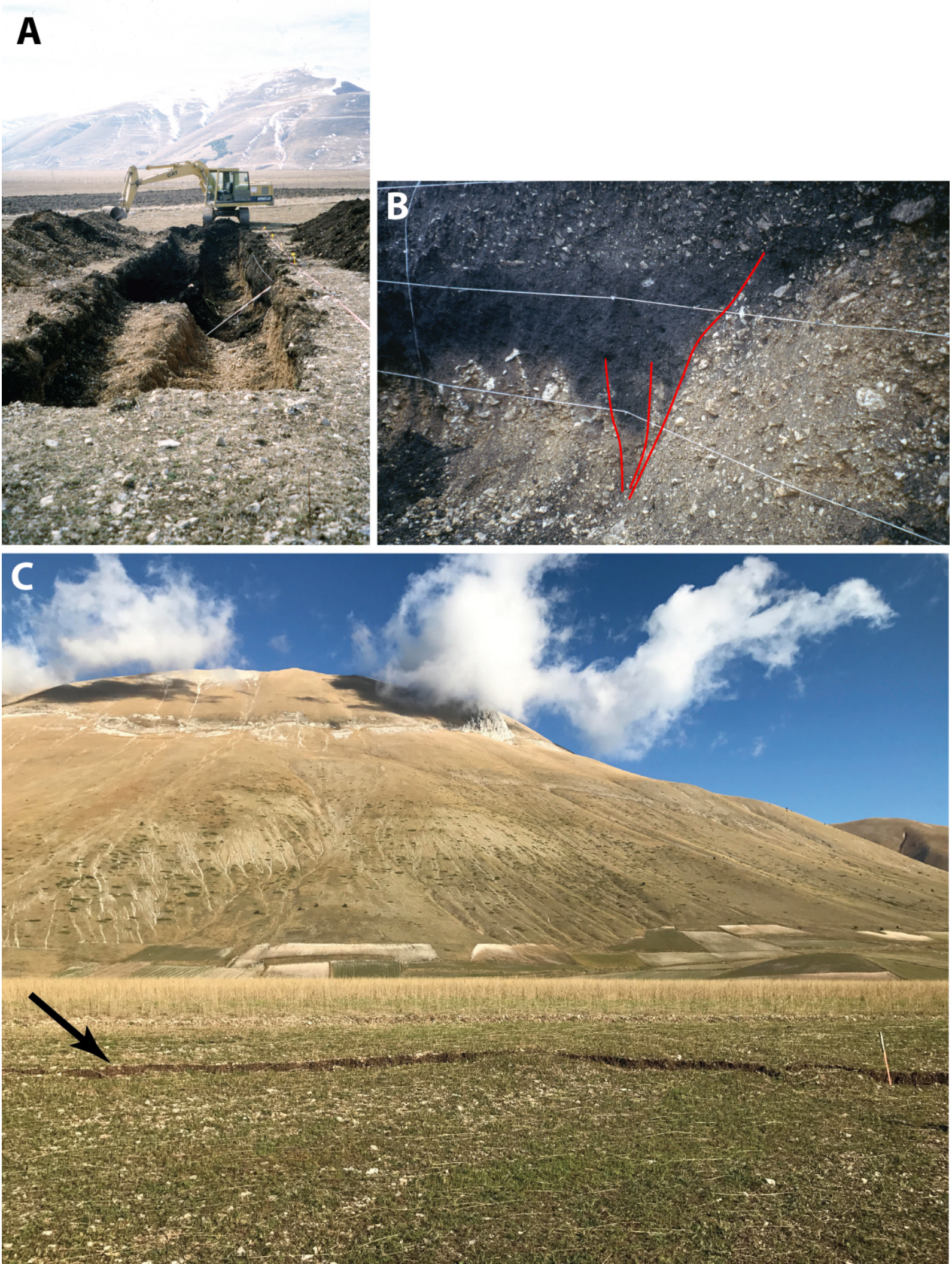
A
B
C

A

B

C

D

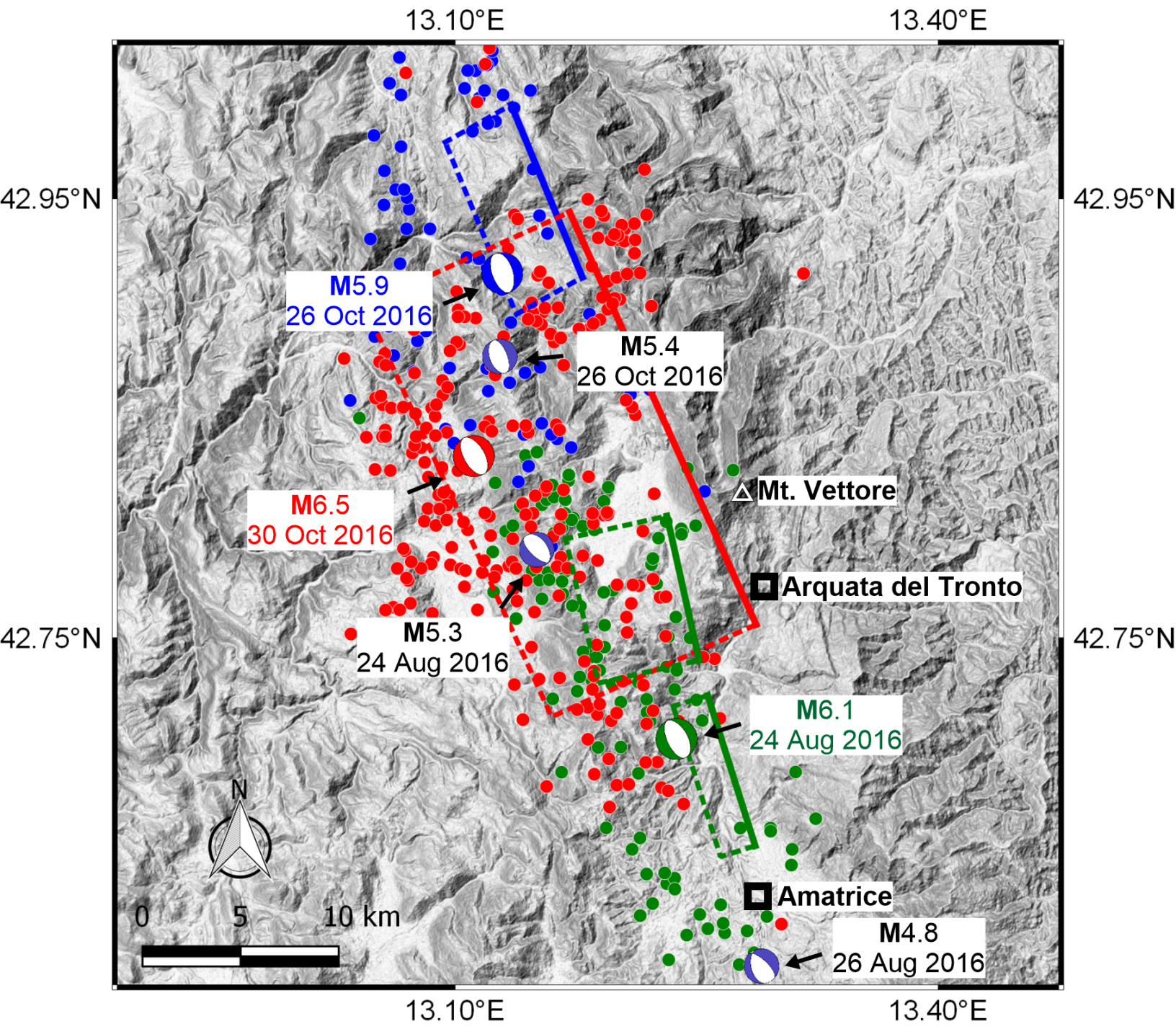
13.10°E
13.40°E
42.95°N
42.75°N
M5.9
26 Oct 2016
M5.4
26 Oct 2016
M6.5
30 Oct 2016
M5.3
24 Aug 2016
M6.1
24 Aug 2016
M4.8
26 Aug 2016
Mt. Vettore
Arquata del Tronto
Amatrice
N
0
5
10 km
Trimmed finite fault model 24 August
Trimmed finite fault model 26 October
Trimmed finite fault model 30 October
Aftershocks 24 August
Aftershocks 26 October
Aftershocks 30 October

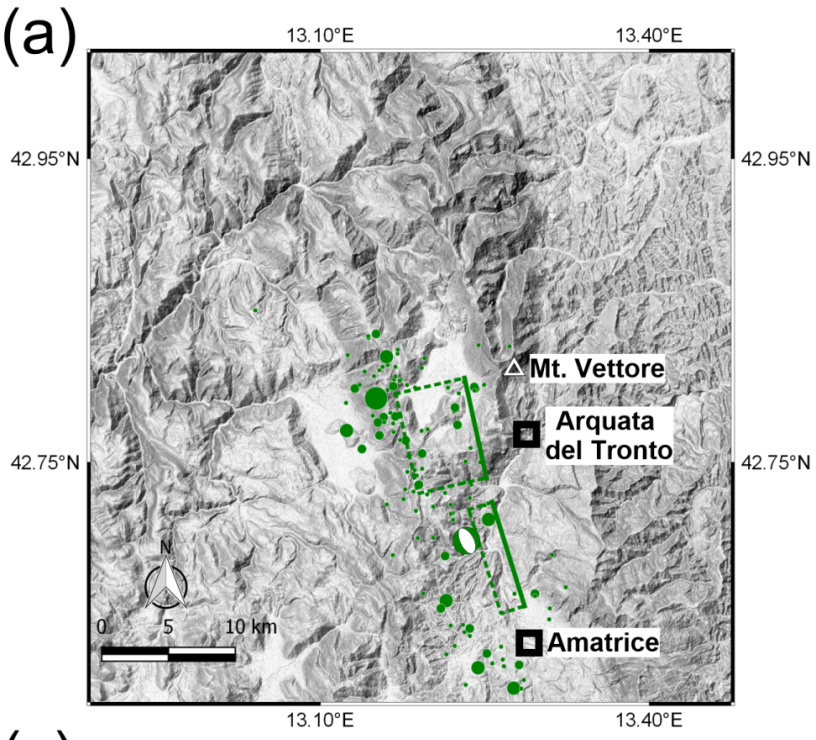

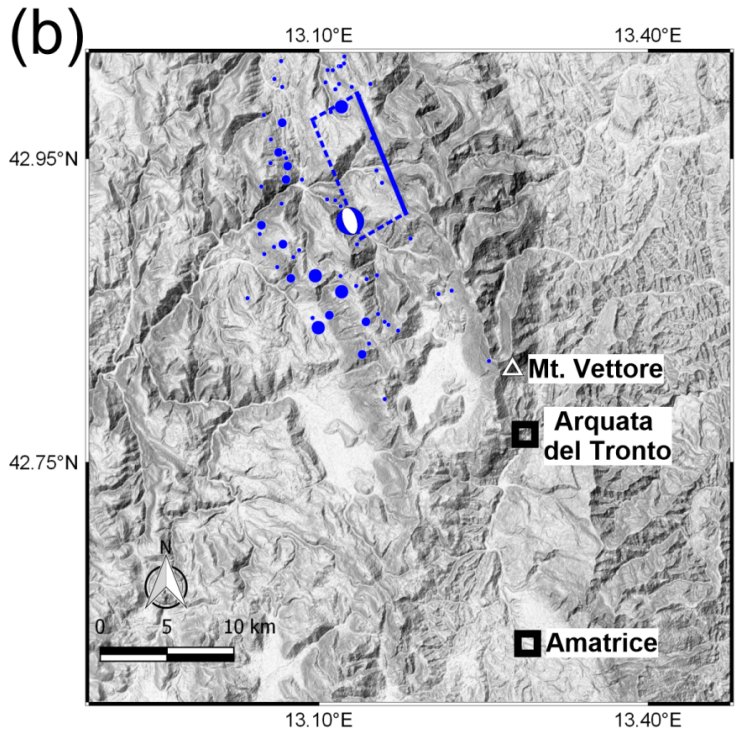

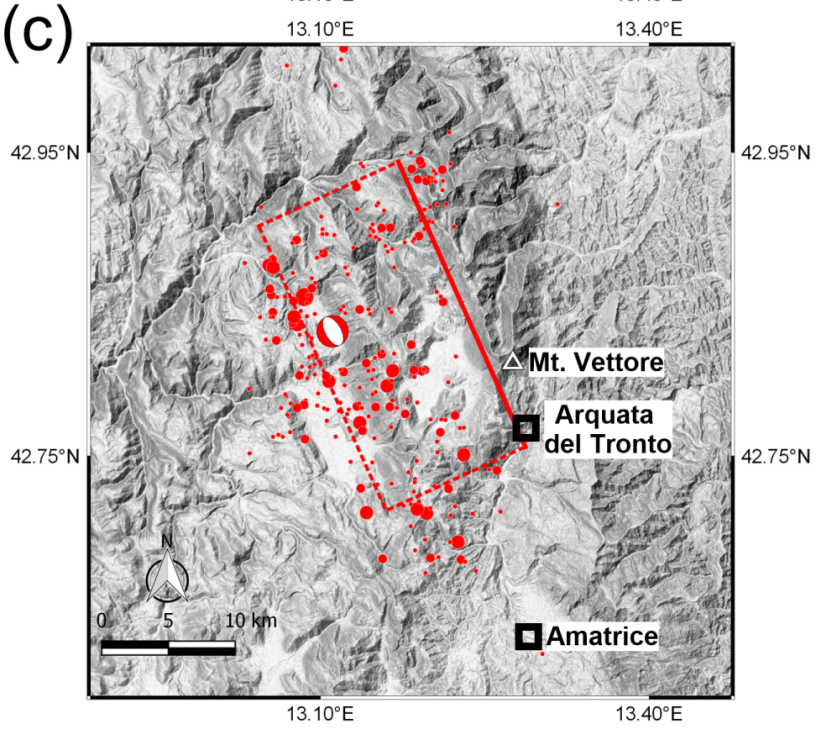

Magnitude (**M**)

- 3.0 - 3.5
- 3.5 - 4.0
- 4.0 - 4.5
- 4.5 - 5.0
- 5.0 - 5.5
- 5.5 - 6.0
- 6.0 - 6.5

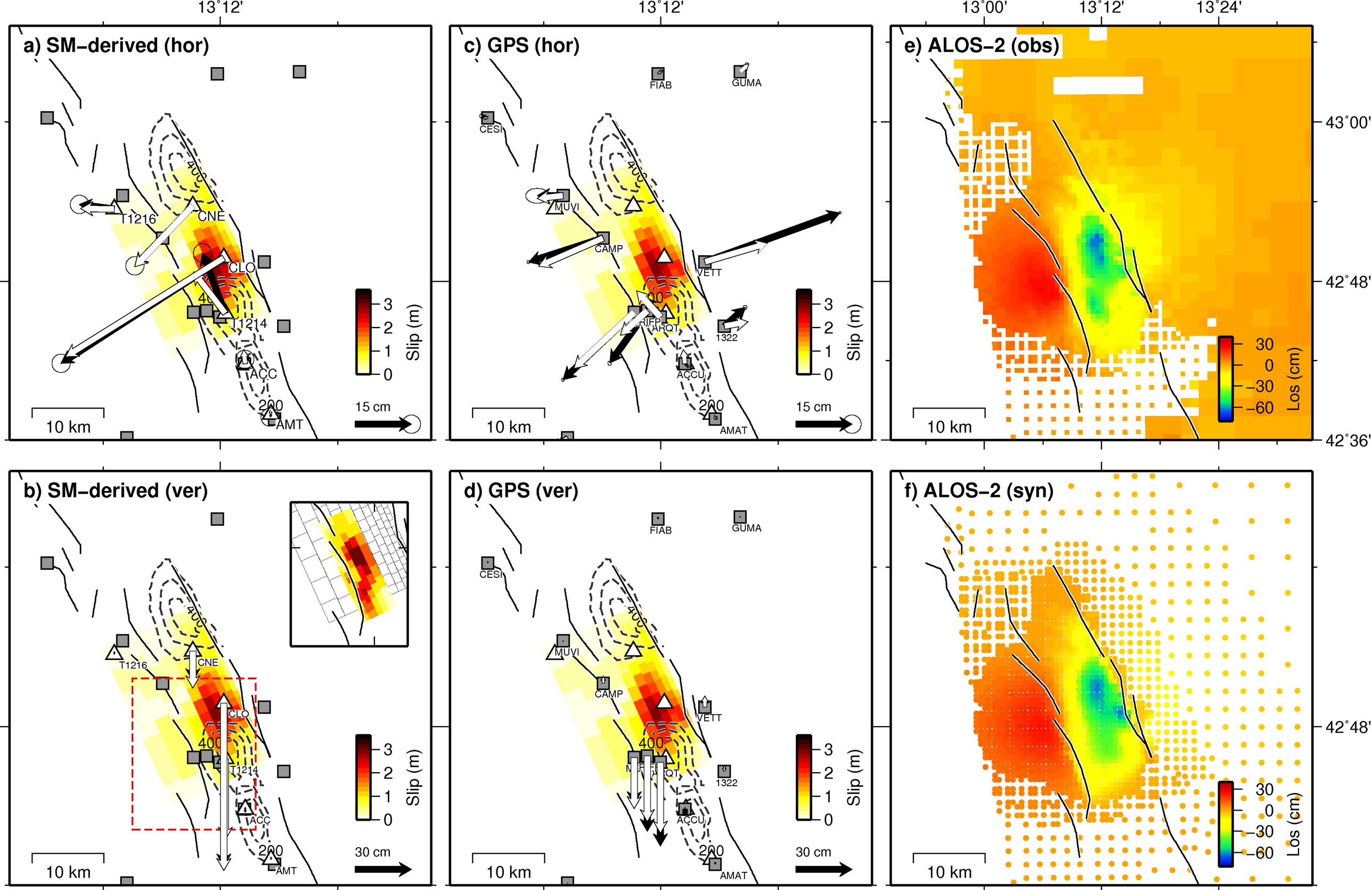
a) SM–derived (hor)
b) SM–derived (ver)
c) GPS (hor)
d) GPS (ver)
e) ALOS–2 (obs)
f) ALOS–2 (syn)
13°12'
13°00'
13°24'
43°00'
42°48'
42°36'
T1216
CNE
CLO
T1214
ACC
AMT
FIAB
GUMA
CESI
MUVI
CAMP
VETT
1322
ACCU
AMAT
400
200
10 km
15 cm
30 cm
Slip (m)
Los (cm)
3
2
1
0
30
0
−30
−60

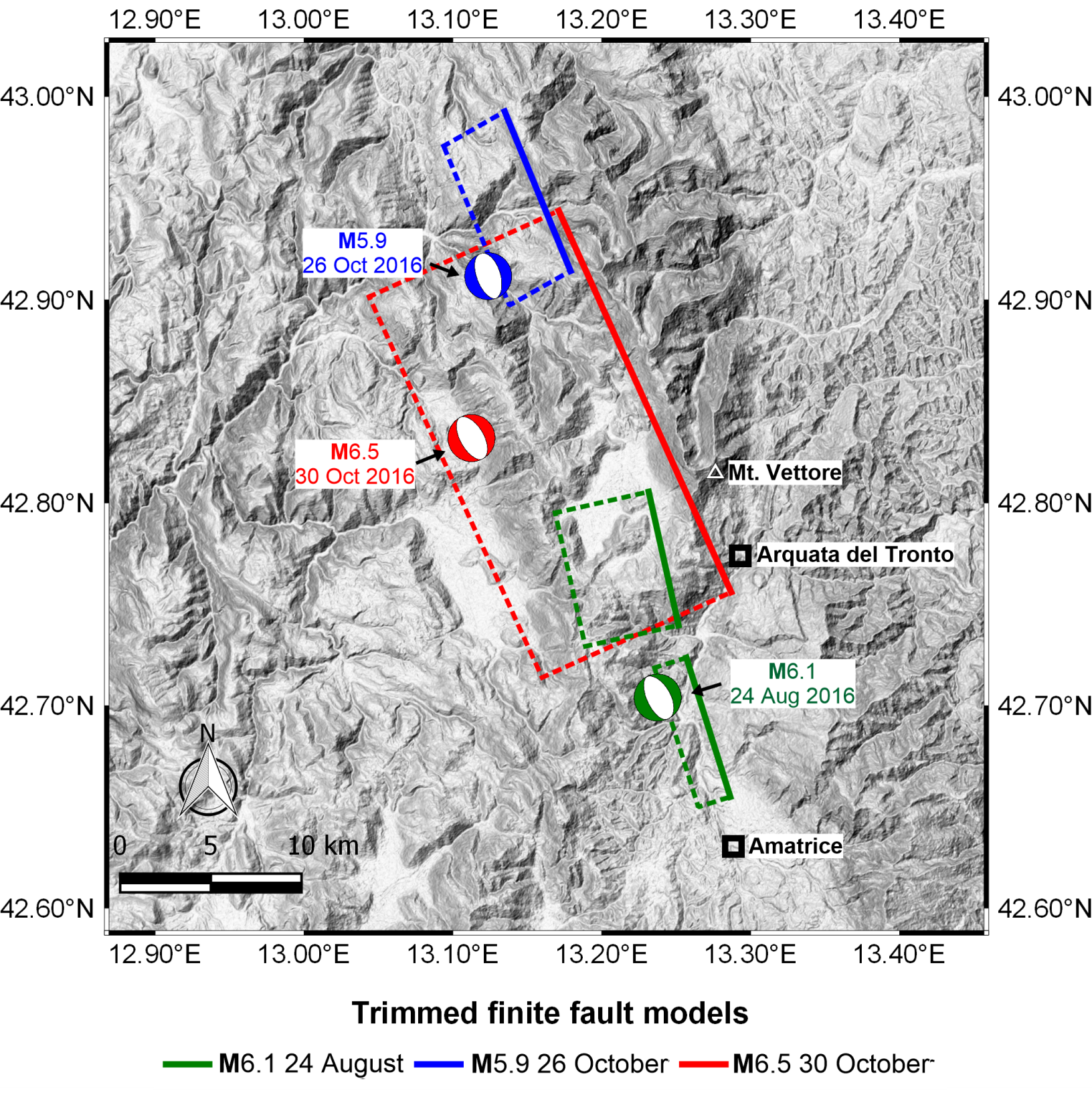

Trimmed finite fault models

M6.1 24 August — **M**5.9 26 October — **M**6.5 30 October